

Introduction to MEMS

[Slides taken and/or adapted from
- a seminar by dr. Cristina Bertoni
- a presentation given to the GE annual meeting
- slides by dr. Valeria Toffoli]



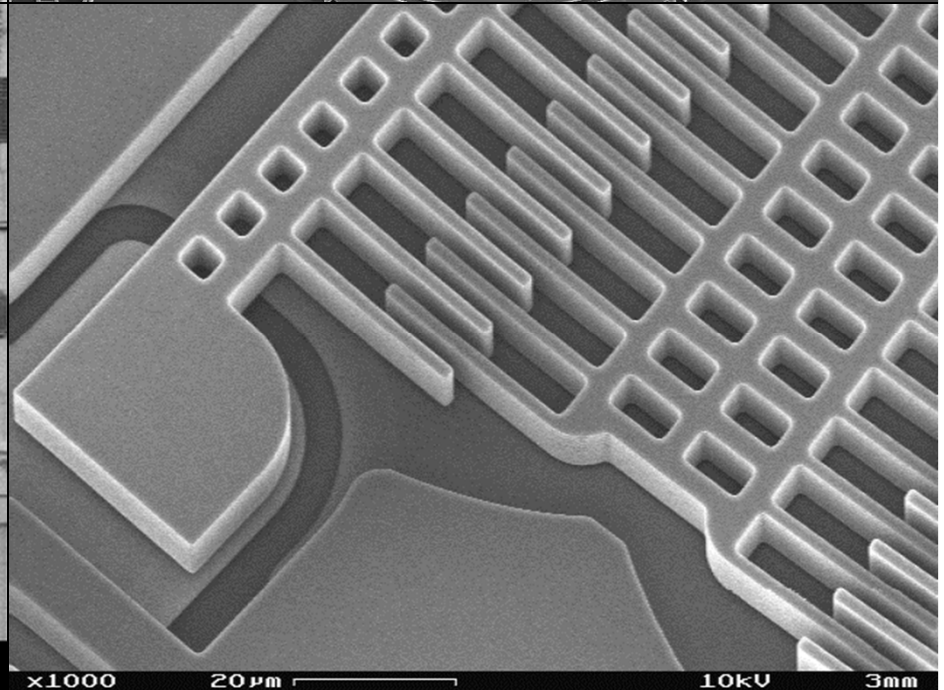
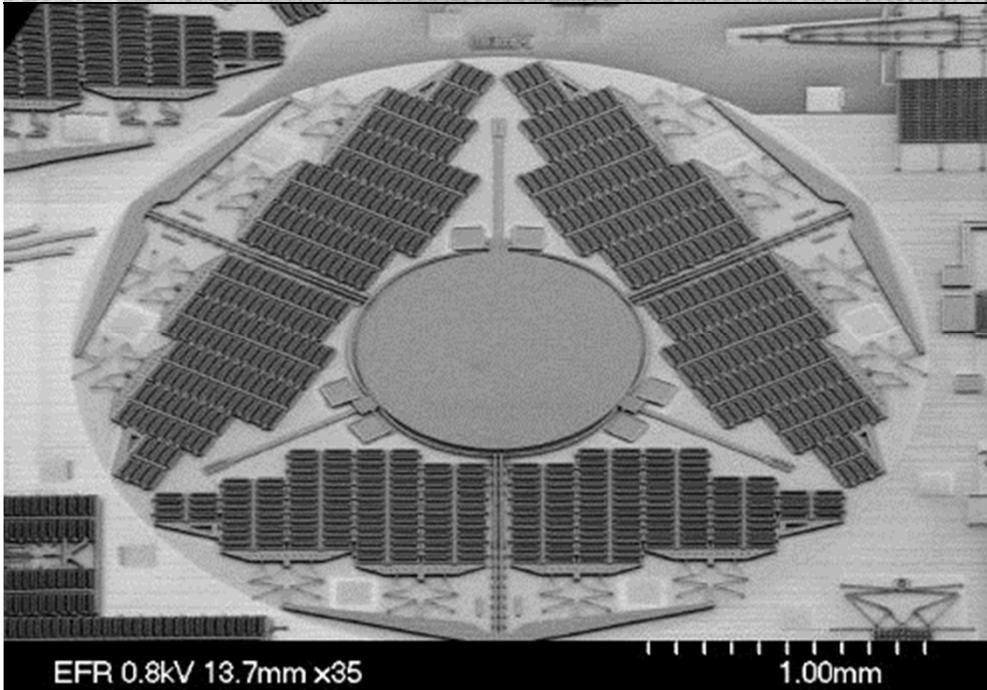
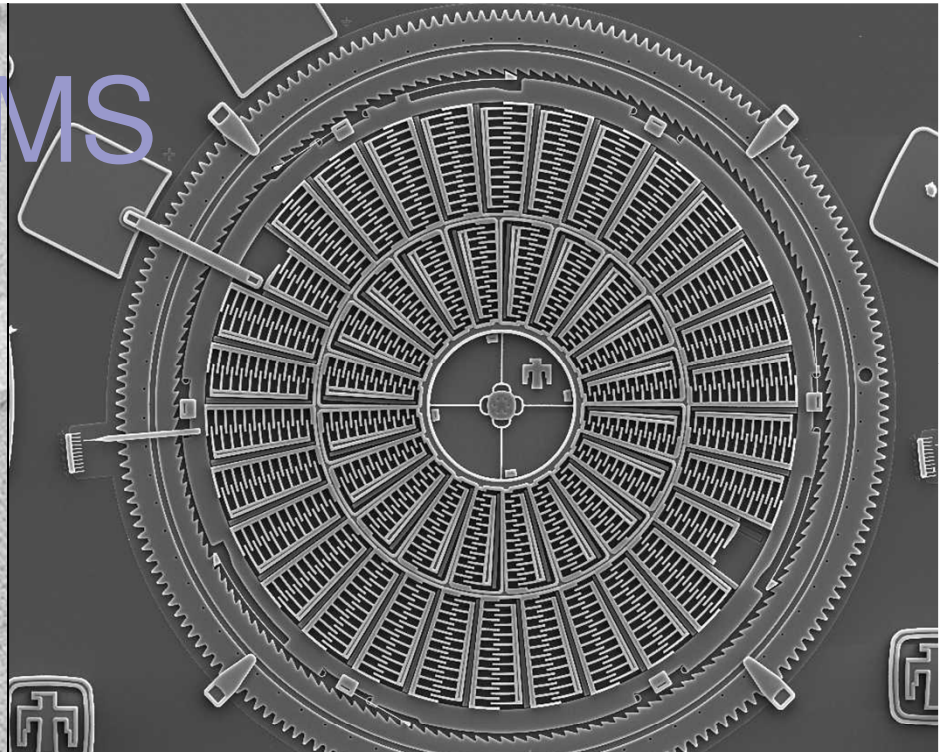
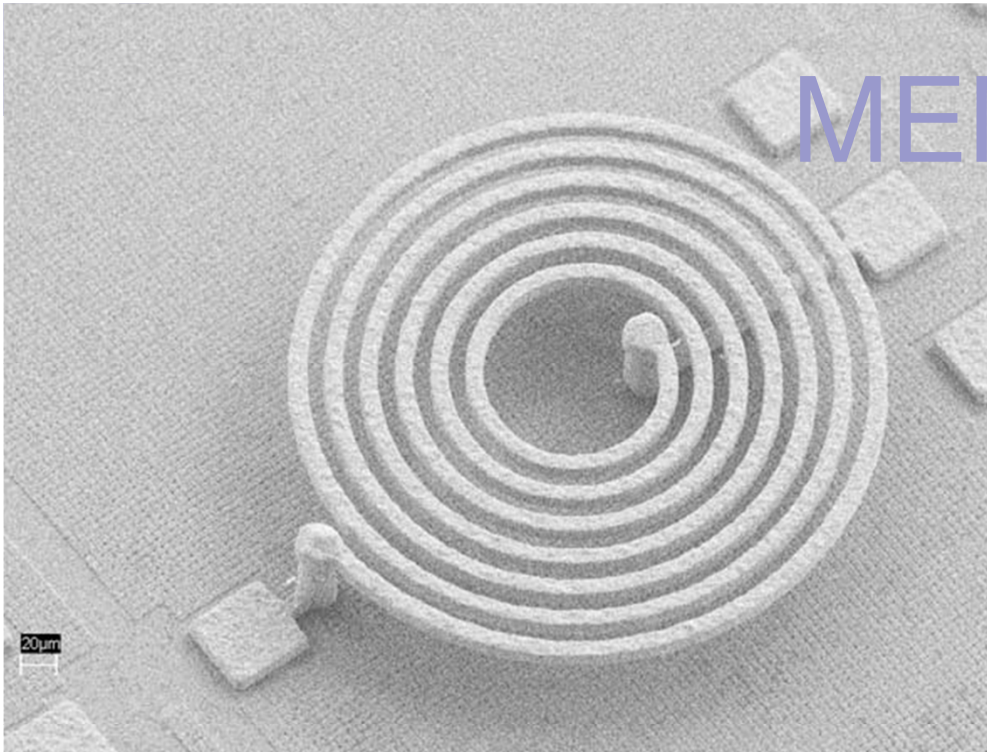
MEMS: micro electro-mechanical systems

- Silicon integrated circuit industry is able to produce devices in volume with **very high yield** at **low cost**
- Silicon has driven the semiconductor industry and allowed for progressive **reduction in size** for more than 3 decades

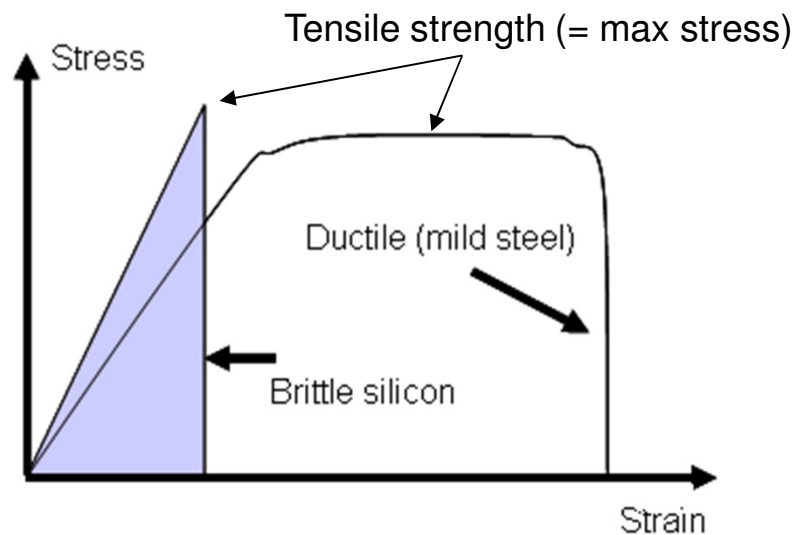
In **MEMS**:

- ✓ Silicon technology is **well-established**
- ✓ Possibility of **integration** with microelectronics on a single chip

MEMS



Mechanical properties of silicon



- Single-crystal Si (SCS) is almost a perfect material: **dislocations in SCS < metals**
- Materials usually deform above yield stress and fails completely at the ultimate stress
- in metals, ultimate stress \gg yield stress
- in **silicon, yield stress \sim ultimate stress**

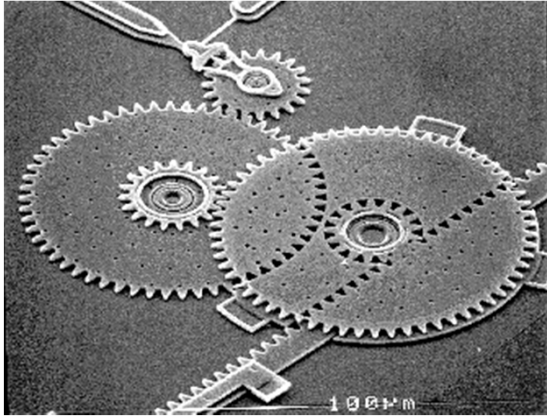
- SCS exhibits no plastic deformation or creep up to 800 °C and so it has an **intrinsic mechanical stability**
- **No fatigue failure** when subject to a high number of cycles
- Absence of plastic behavior means that resonating structures of **exceedingly high Q** can be made



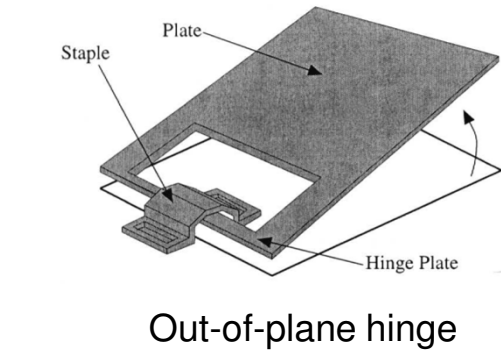
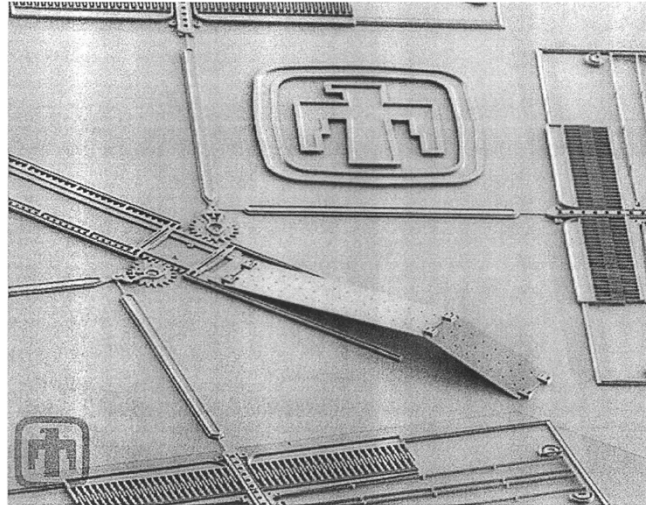
	Yield Strength (GPa)	Young's Modulus (GPa)	Density (g/cm ³)	Thermal Conductivity (W/cm °C)	Thermal Expansion (ppm/°C)
Diamond	53	1035	3.5	20	1
SCS	>1	180	2.3	1.6	2.3
Steel	4.2	210	7.9	1.0	12.0
Aluminium	0.2	70	2.7	2.4	25

- Thermal expansion coefficient very important in packaging
- Remember that silicon properties depend on the direction in the crystal lattice, i.e. tensors may be required
- SCS Fracture Strength > 1.0 GPa

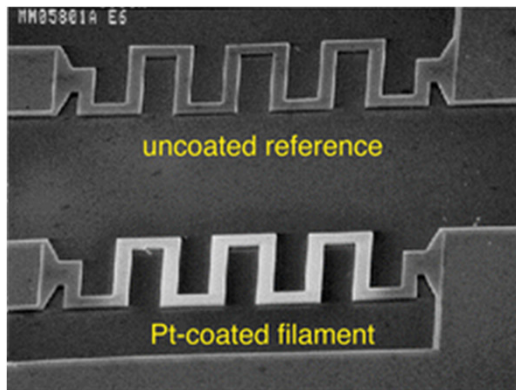
Other MEMS structures...



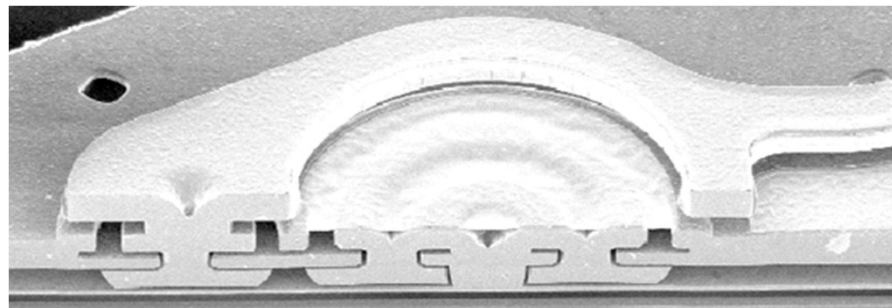
Microtransmission



Micromirror



Catalytic microsensor

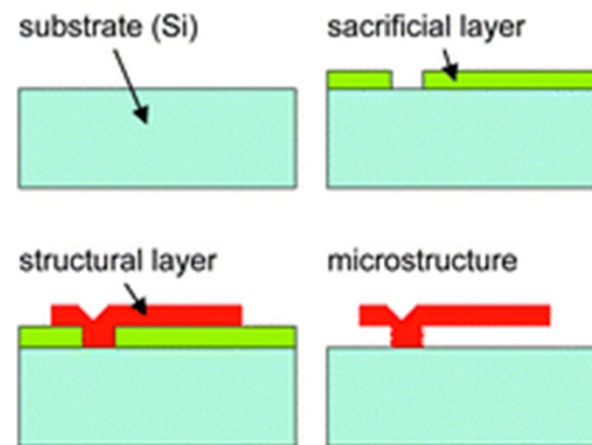
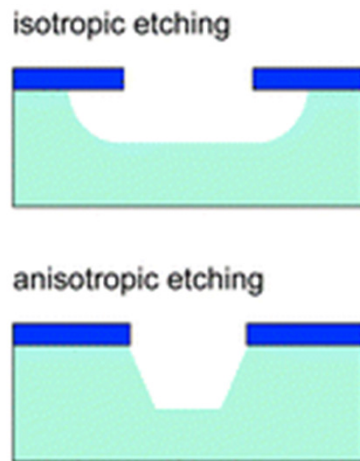


3-levels device cross-section

Silicon micromachining

Most MEMS fabrication techniques can be classified as

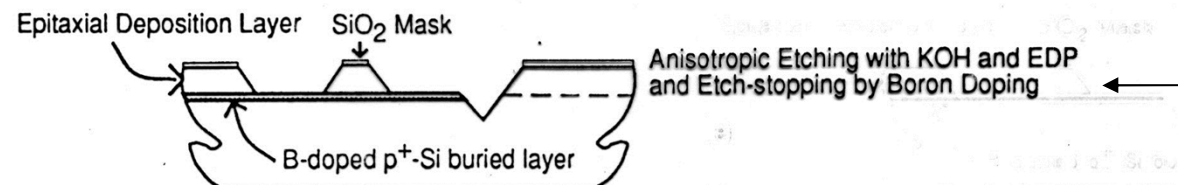
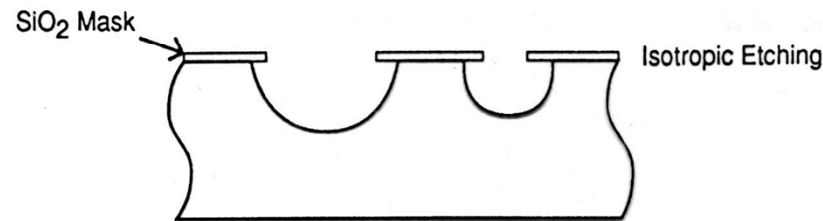
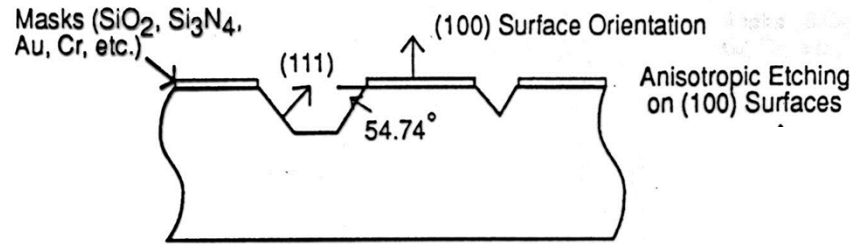
- *in* the substrate, **bulk micromachining**, or
- *above* the substrate, **surface micromachining**.



Bulk micromachining is a fabrication technique to selectively remove substrate to create MEMS devices

Surface micromachining is a fabrication technique for depositing various films on top of the substrate (substrate as a construction base material) and selectively remove parts of deposited films to create MEMS devices

Wet etching

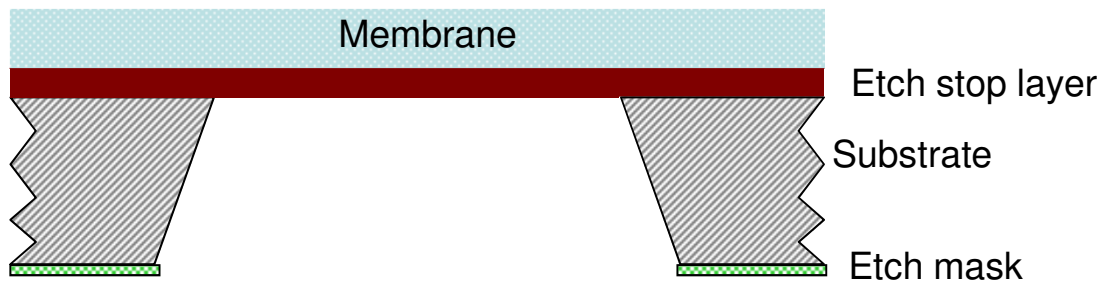


KOH (potassium hydroxide) is frequently used for **anisotropic etching**: the (111) surface direction of silicon crystal is etched at a very low speed compared with (100). Therefore, a (100) silicon wafer surface can be etched by KOH etchant with 54.74 deg slopes.

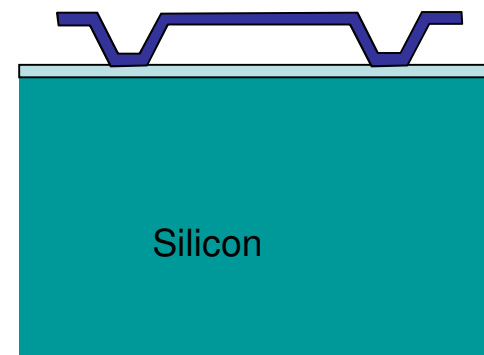
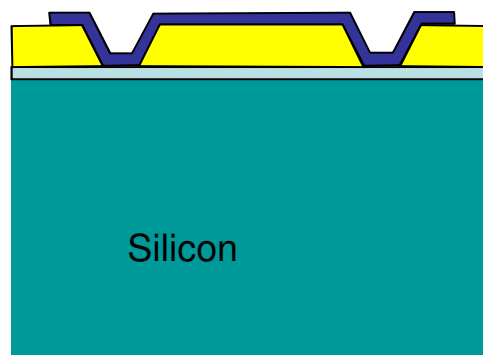
HNA ($\text{HF} + \text{HNO}_3 + \text{CH}_3\text{COOH}$) is commonly used as an **isotropic etchant**: the etching speed does not depend upon the crystal axis

A deeply doped silicon layer can be used as an etch-stop layer.

Approaches for the fabrication of membranes

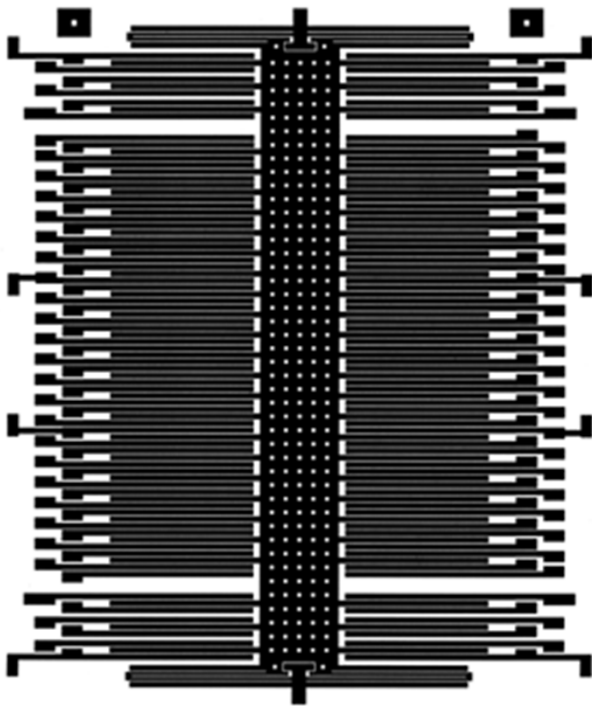


-  Sacrificial Layer
-  Bridge Layer
-  Oxide Layer

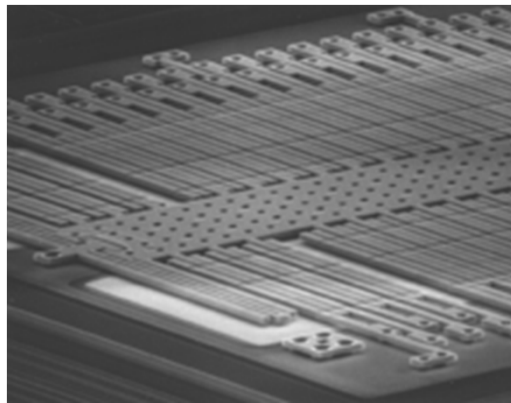


IC + MEMS integration

- Typical MEMS/IC integration is done by fabricating **IC first**
- MEMS is post-processed on top of IC or pre-designated MEMS area on the IC

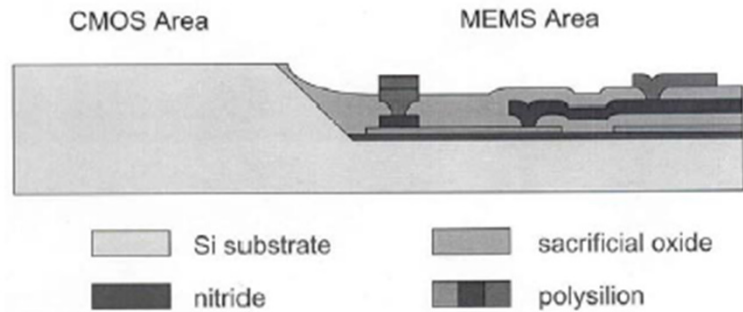


- Proper IC protection is needed
- Post-IC process temperature cannot exceed 450°C to avoid IC degradation
 - redistribution of dopants
 - inter-diffusion of materials



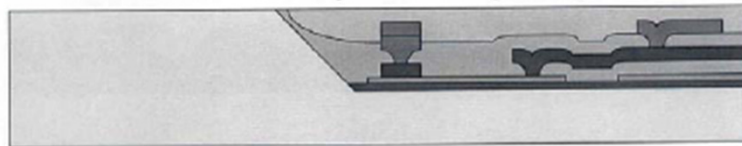
Analog devices ADXL-50, the industry first surface micromachined accelerometer including signal conditioning on chip

IC + MEMS integration

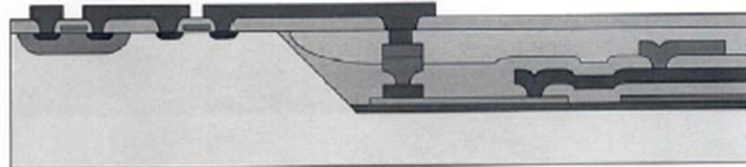


MEMS first approach developed at Sandia Labs

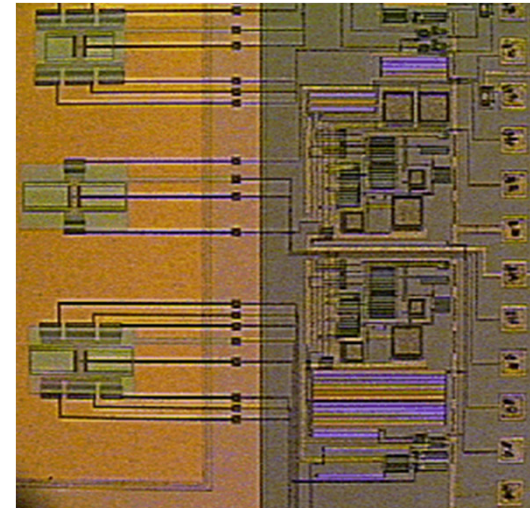
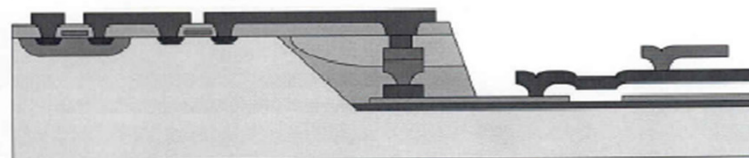
- fill trench with oxide, planarize (CMP)



- standard CMOS device fabrication



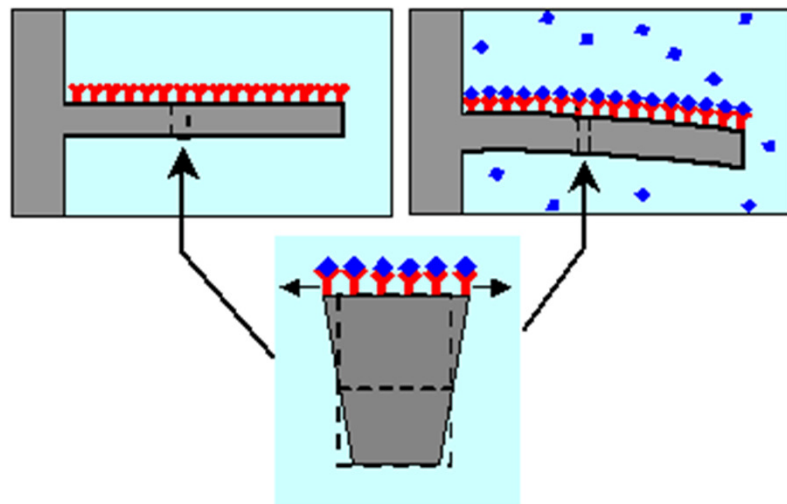
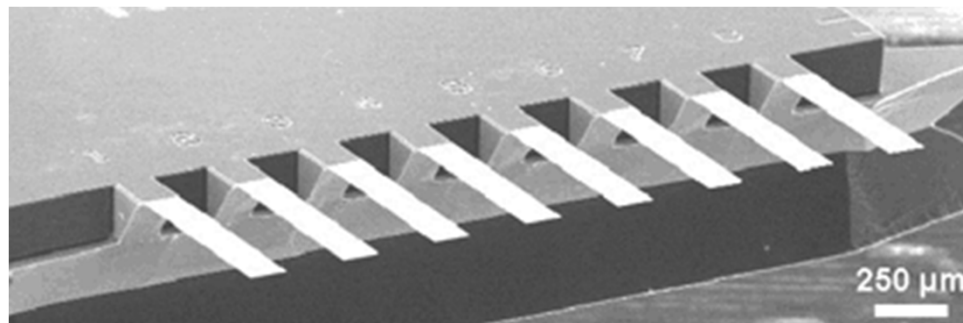
- etch sacrificial oxide in MEMS area



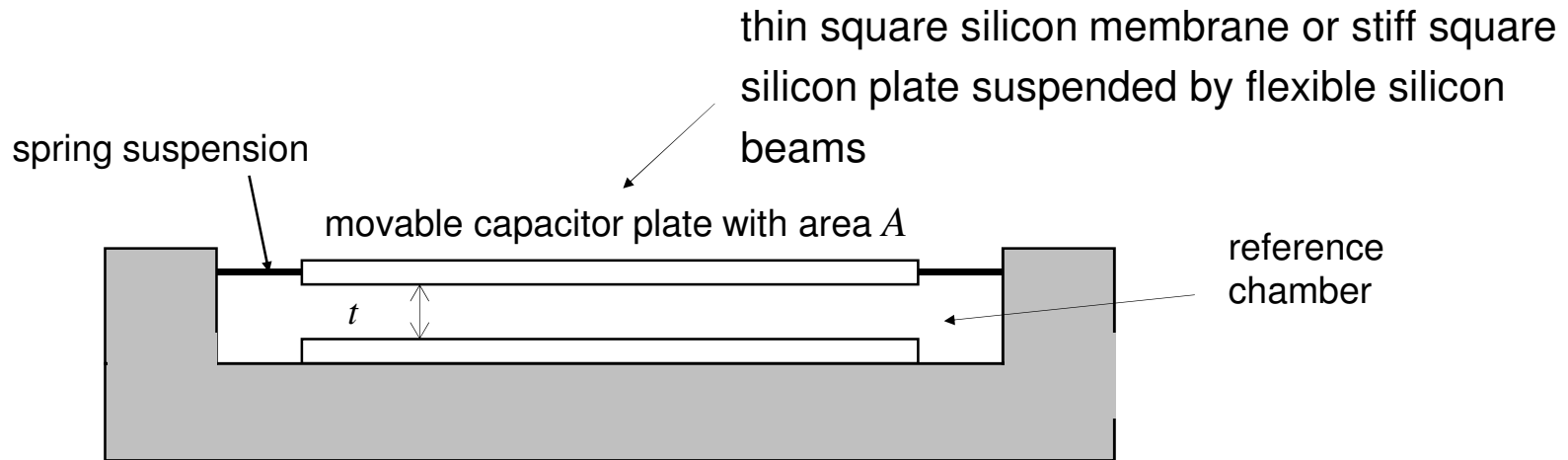
<http://mems.sandia.gov/tech-info/mems-overview.html>

Cantilevers

- Widespread application in atomic force microscopy
- Biological and chemical sensors



Capacitors in MEMS



Use a capacitor with one fixed plate and one moving plate to give a variable capacitance

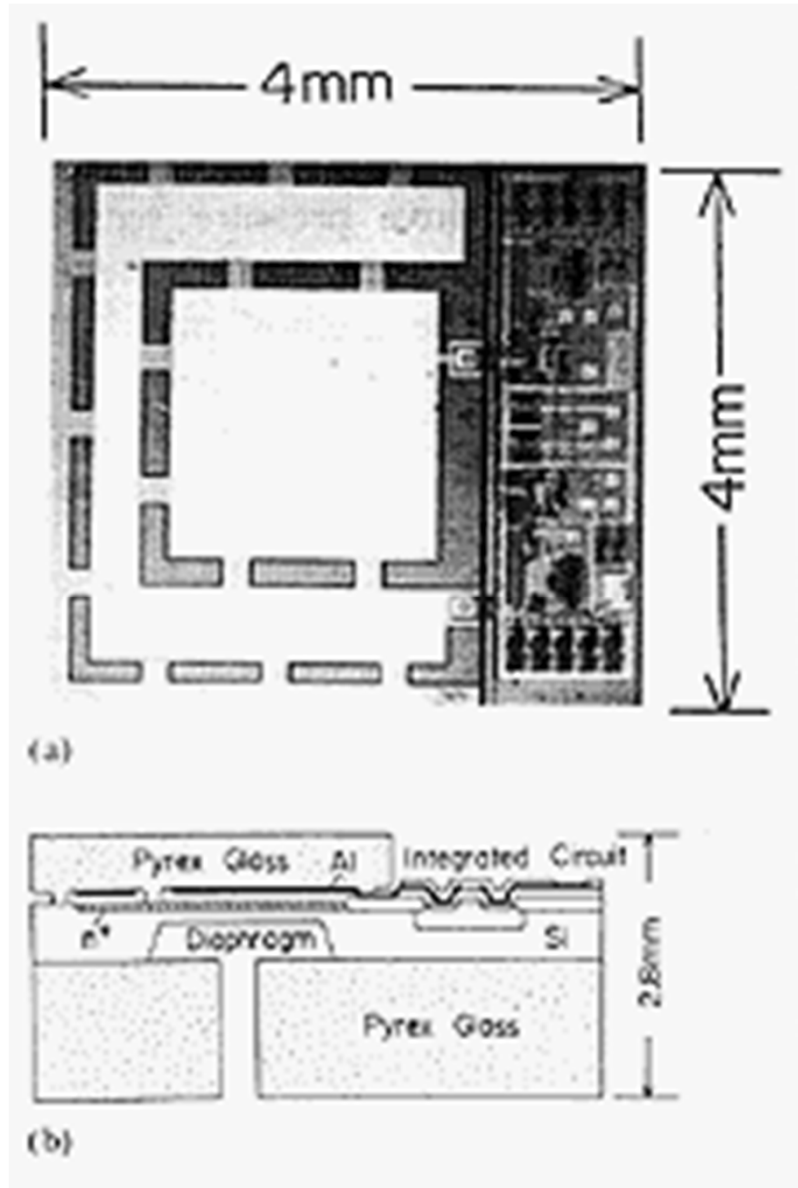
$$C = \epsilon_0 \epsilon_r \frac{A}{t}$$

(for a N_2 filled capacitor $\epsilon_r \sim 1$)

if $\Delta t \ll t$, the sensitivity to Δt is

$$\frac{\Delta C}{\Delta t} = -\epsilon \frac{A}{t^2}$$

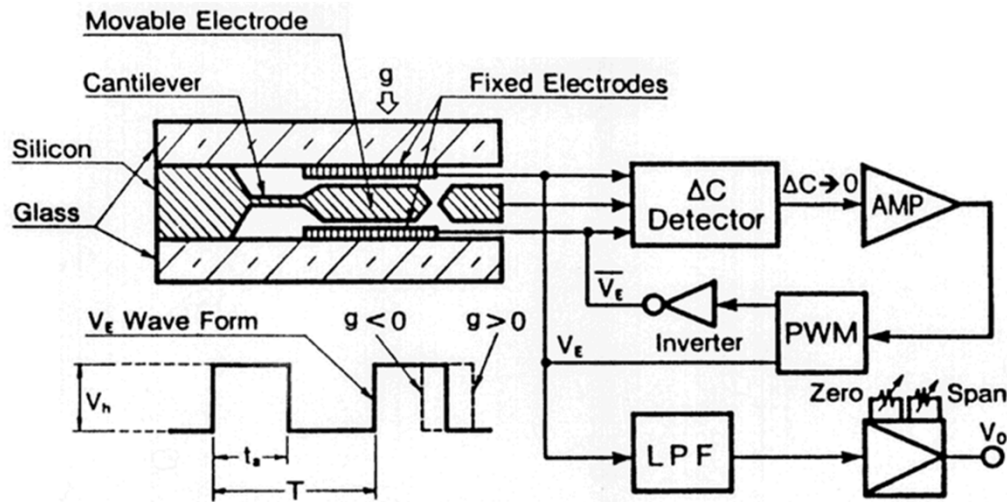
Examples of capacitors in MEMS



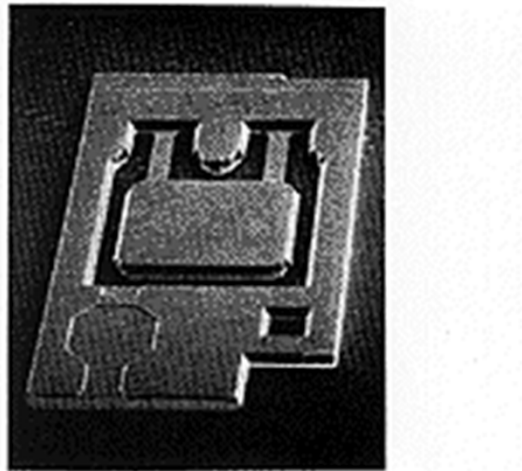
Photograph (top) and cross sectional diagram (bottom) of ***Toyota capacitive pressure sensor*** – employs bulk micromachining

Ref: www.tec.org/loyola/mems/c3_s2.htm

Examples of capacitors in MEMS



(a)



(b)

Cross section & block diagram (top) and photograph (bottom) of **Hitachi capacitive accelerometer** – employs bulk

micromachining

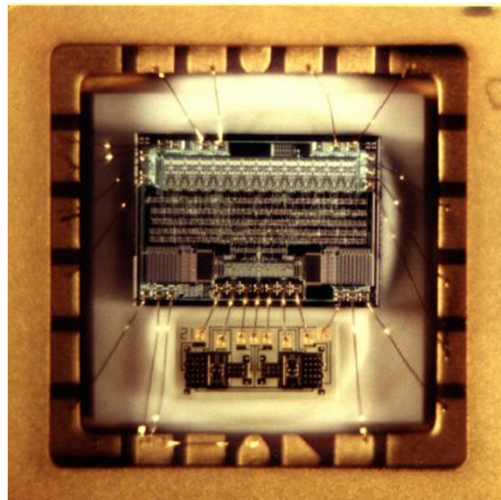
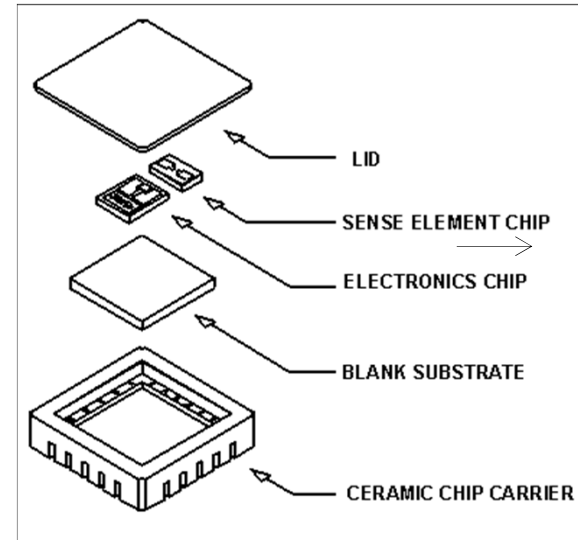
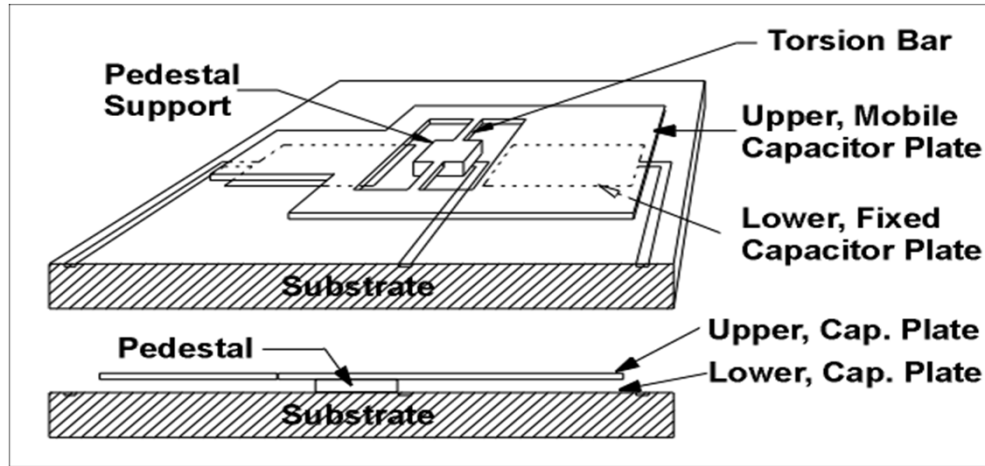
AMP = amplification

PWM = pulse width modulator

LPF = low-pass filter

Ref: www.tec.org/loyola/mems/c3_s2.htm

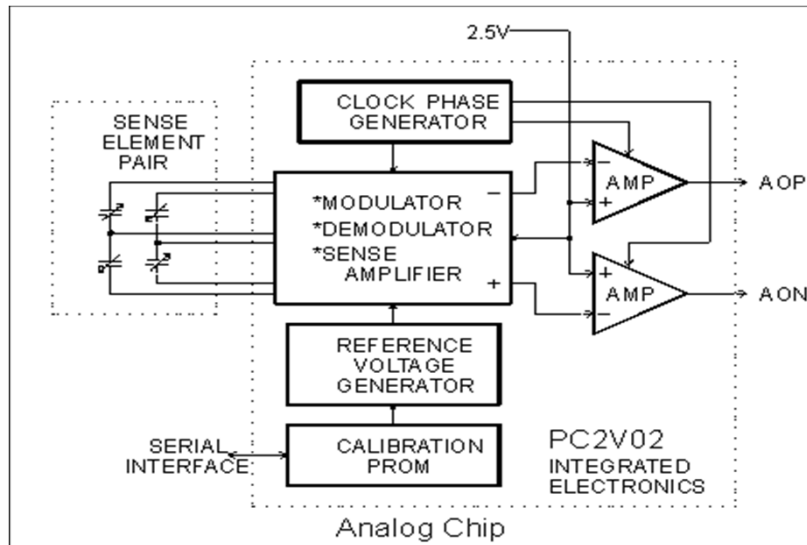
Examples of capacitors in MEMS



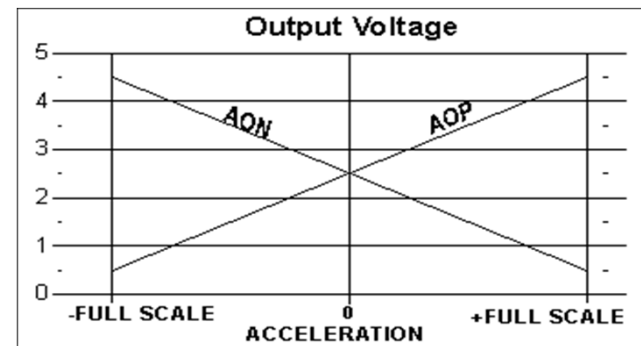
Silicon Designs Inc (SDI) torsional accelerometer uses an electroformed nickel structure

Ref: <http://www.silicondesigns.com/tech.html>

Examples of MEMS capacitor sensor circuits



Analogue ASIC for SDI accelerometer: it is basically a capacitance-to-voltage converter



The electronics produces a large voltage deviation (± 4 volts) that is linearly proportional to the applied acceleration

The output is measured differentially as AOP-AON

Inductors for RF MEMS

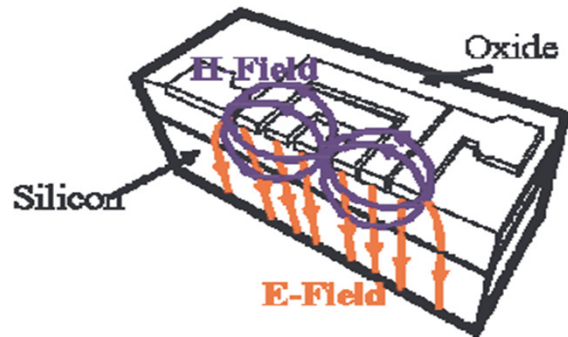


Figure 1. Planar inductor [8].

Planar inductors fabricated on substrates such as silicon suffer from many unwanted stray components that can compromise device performance. Stray capacitances tend to decrease the self-resonance while the conductivity of the substrate tends to reduce the Q-factor. Typical $Q < 10$, $f_r < 1$ GHz.

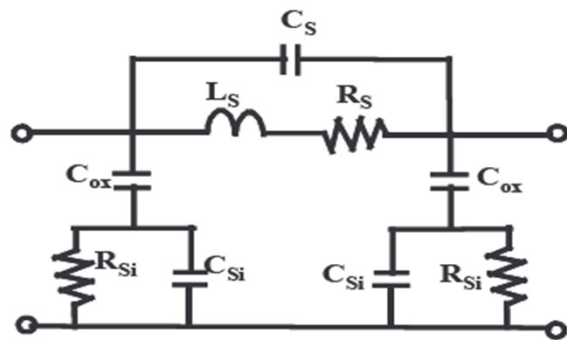
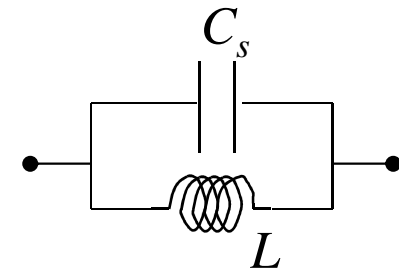
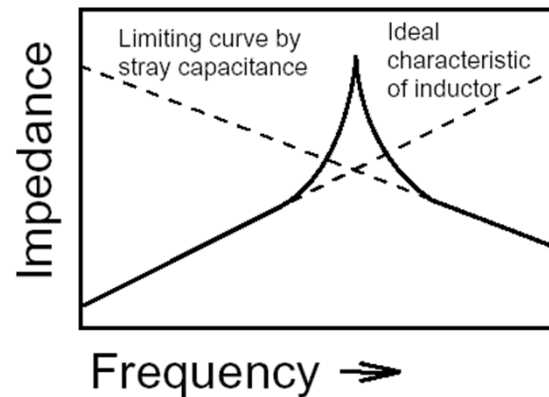
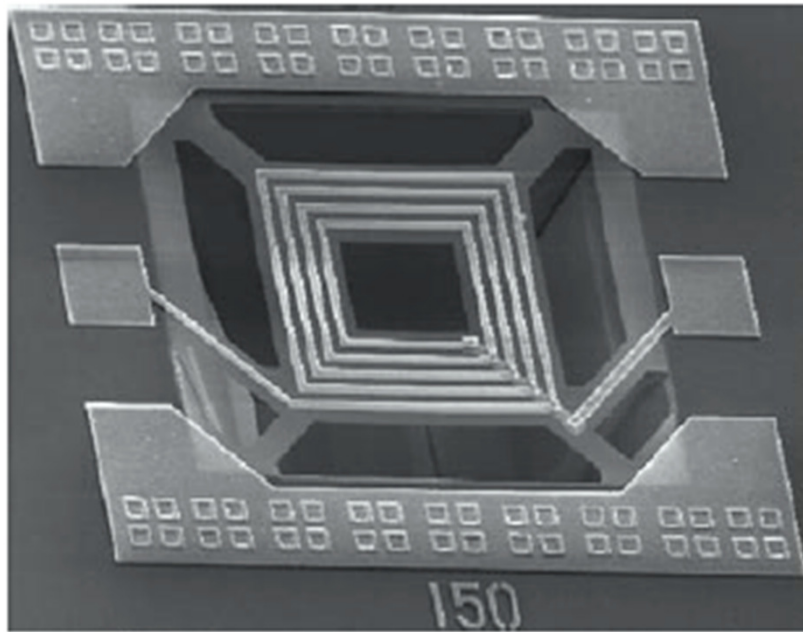


Figure 2. Equivalent circuit model of planar inductor

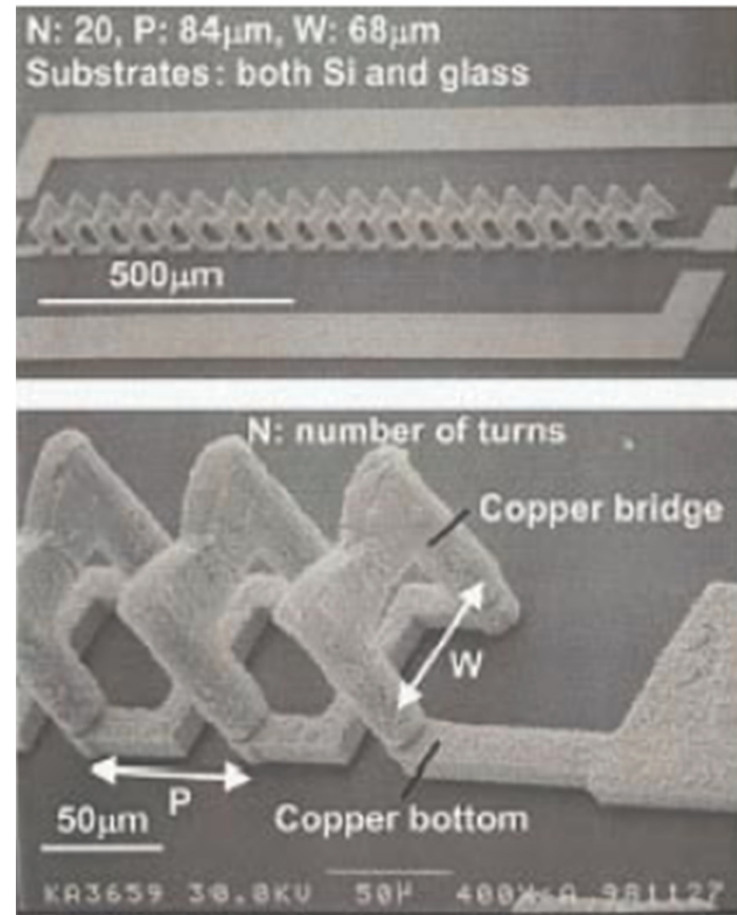
Impedance characteristic



Inductors for RF MEMS



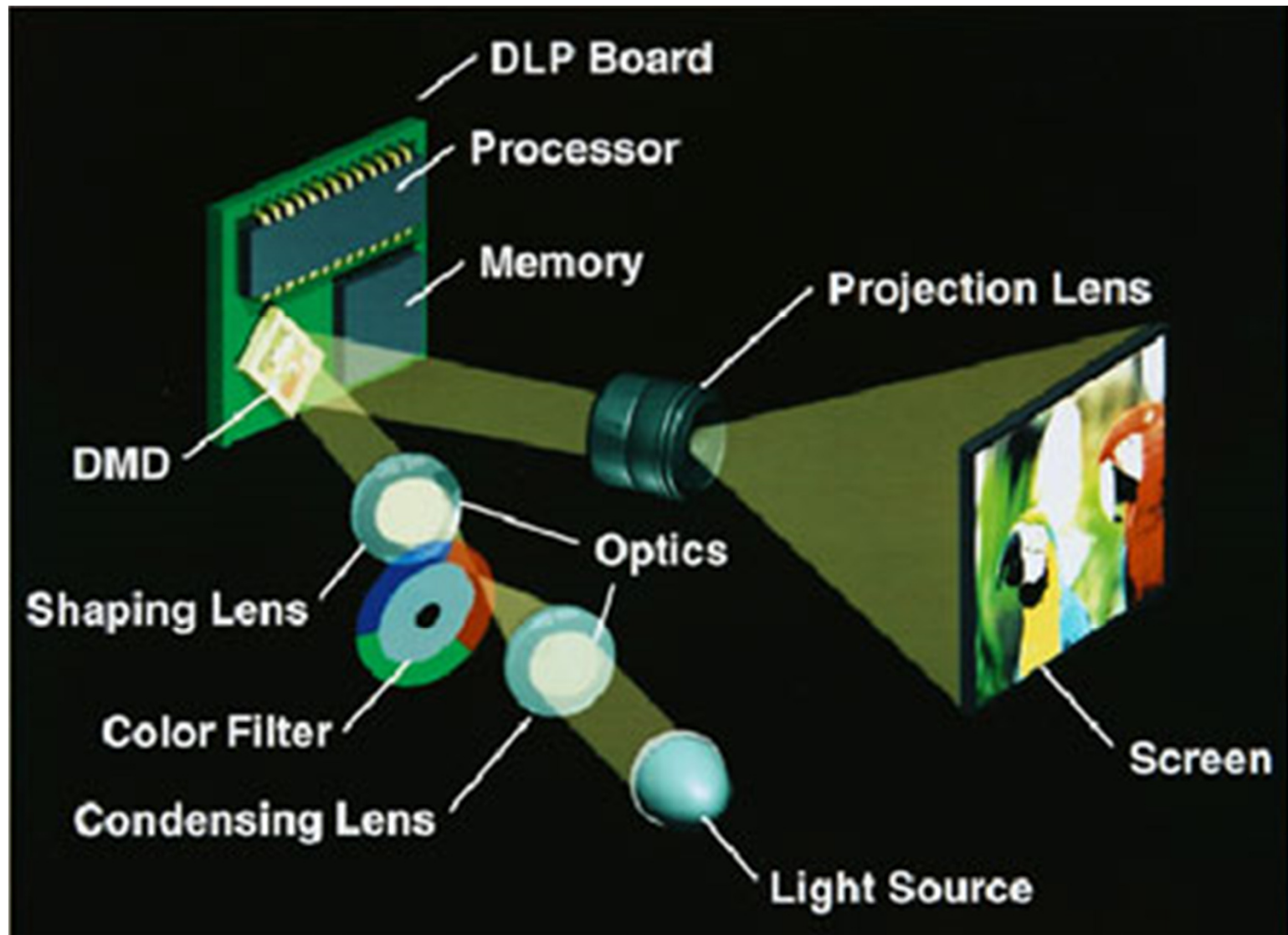
Bulk micromachined planar **spiral** inductor where the substrate has been locally removed from under the turns. Self-resonance f_r is increased from 800 MHz to 3 GHz thanks to substrate removal



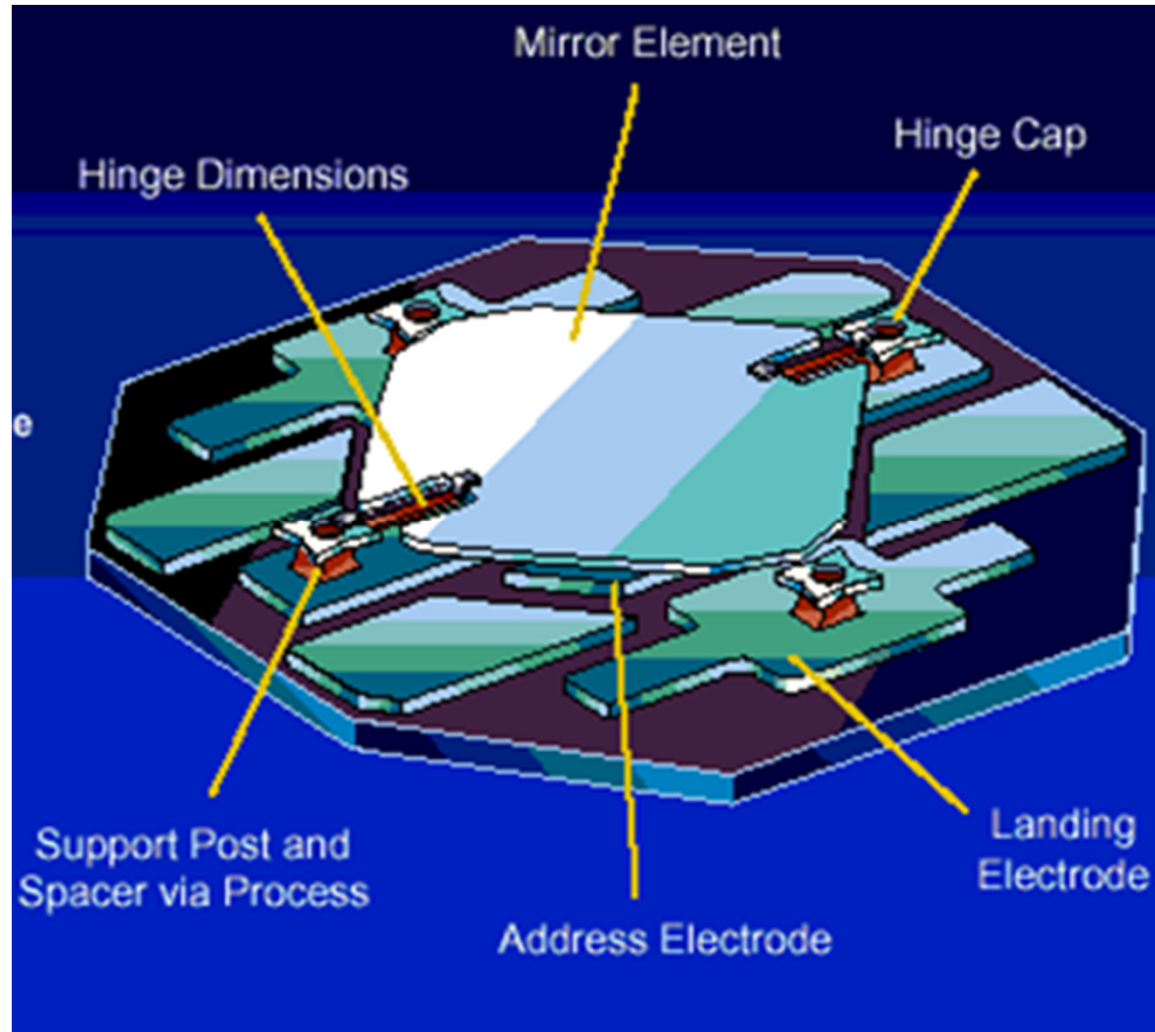
20-turn all-Cu air-core **solenoid** on Si. It reduces parasitic capacitances between metal traces and the substrate

$Q = 16.7$ at 2.4 GHz

TI's DLP technology

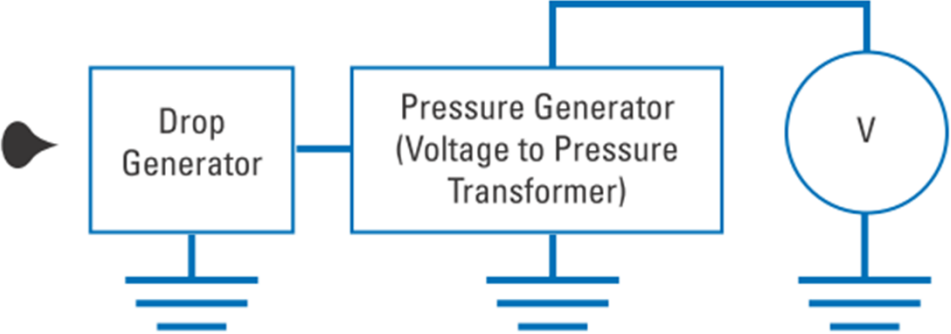


TI's DLP technology

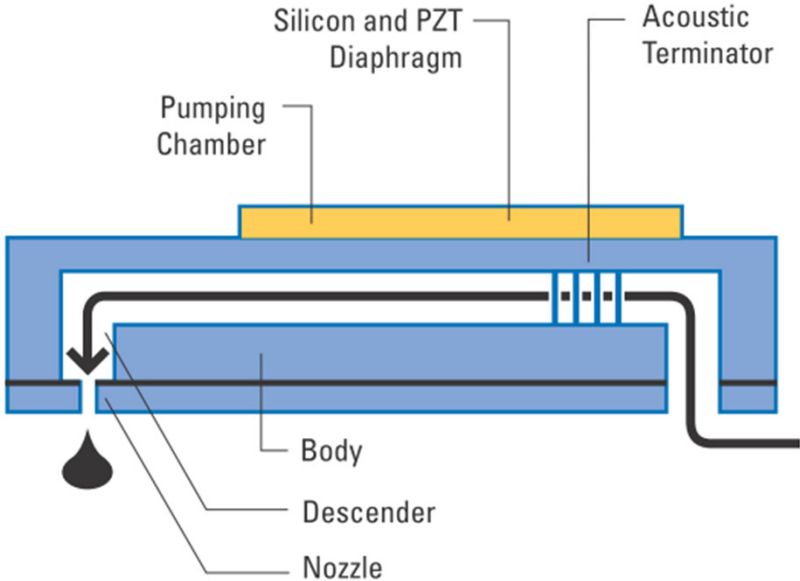


MEMS inkjet printer heads

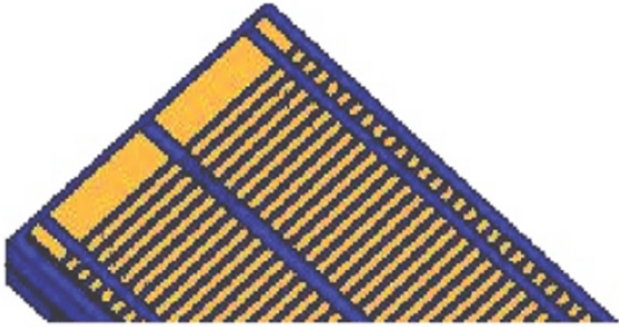
Simplified scheme



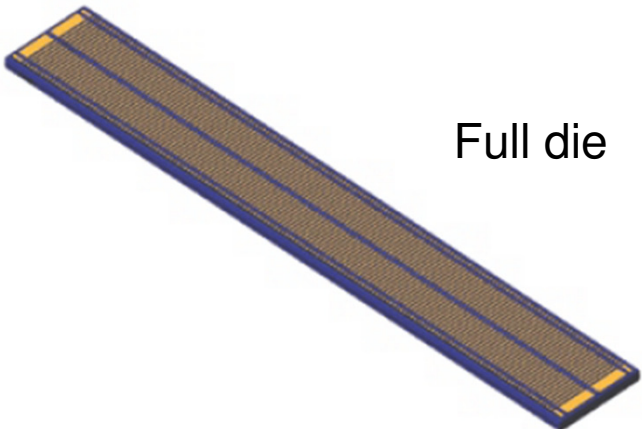
Single jet



Layout of jets on a die



Full die



MEMS inkjet printer heads: processing steps



Figure 2a. Starting Wafer. Begin with a Silicon-on-Oxide (SOI) Wafer.



Figure 2b. Descender/Fill etch. Etch blind holes. This *Descender* will connect the pumping chamber to the nozzle. The *Fill* connects to fluid reservoir.



Figure 2c. Pumping Chamber/Filter Etch. Etch a rectangular pumping chamber with Acoustic Terminator at fill end



Figure 2d. Nozzle/Fill Through Etch. Etch a *through hole* to complete nozzle and fill paths.

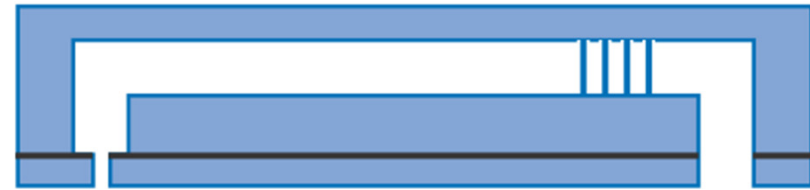


Figure 2e. Actuator Diaphragm Attach. Attach an SOI wafer with a Fusion Bond and remove the handle wafer away to leave a (12 -50 μm) diaphragm.

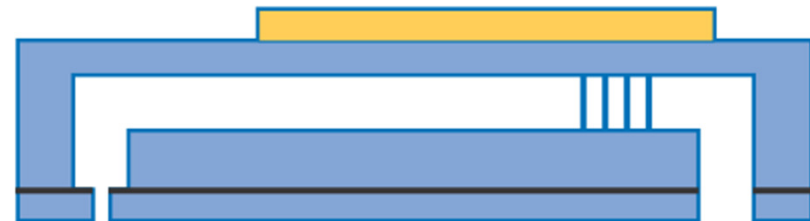


Figure 2f. PZT bond, grind and singulate. PZT, metalized on both sides is bonded to the membrane, ground to its final thickness (1- 50 μm) and sawn to singulate the individual jets.

MEMS inkjet printer heads: details

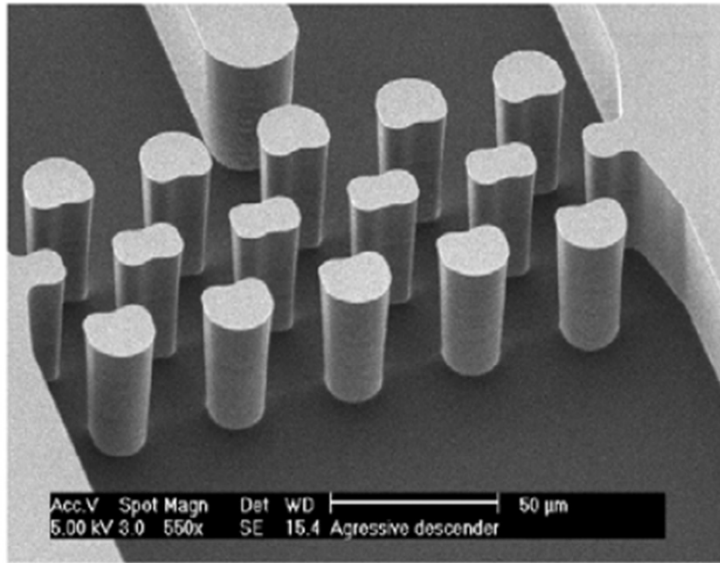


Figure 3a. Acoustic Terminator on fill side of Pumping Chamber

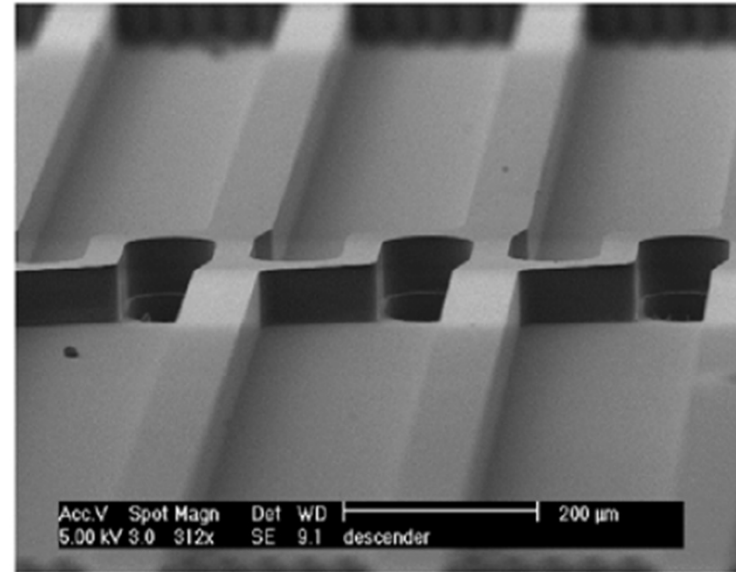


Figure 3b. View toward die center along Pumping Chamber

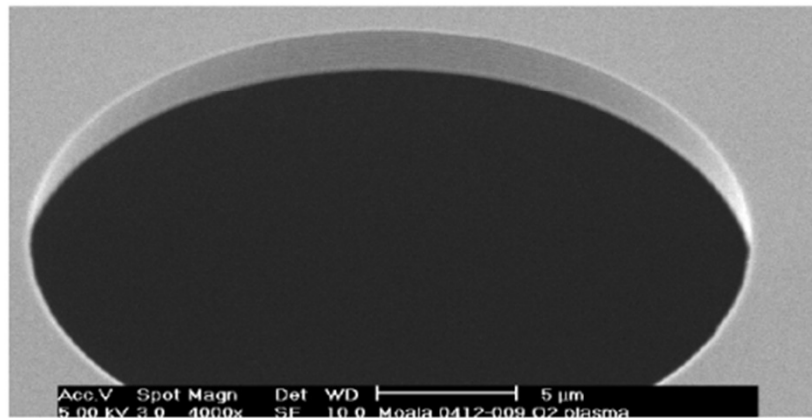
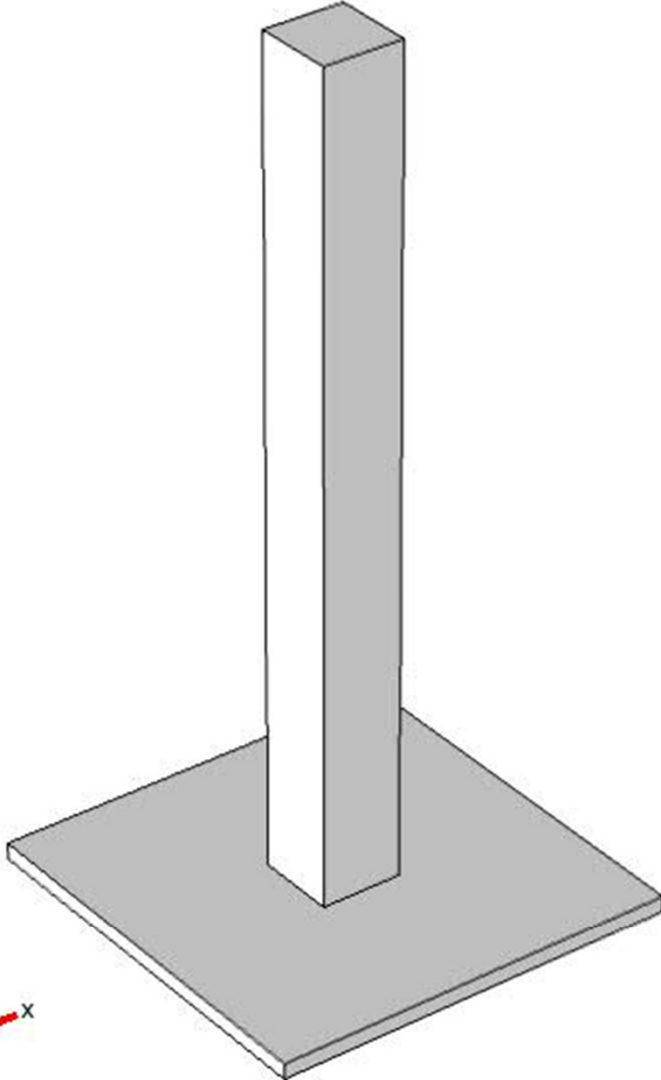
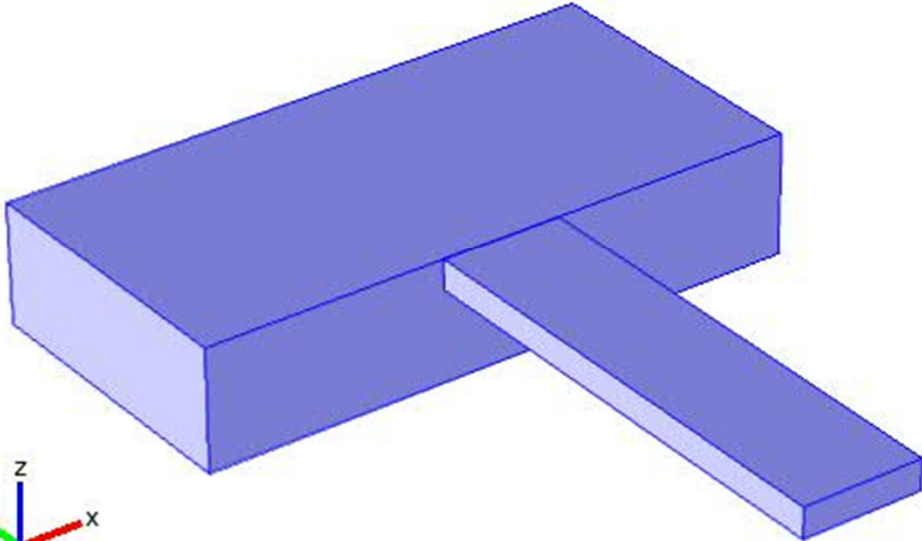


Figure 3c. Nozzle



Cantilevers and pillars





deei



Asymmetrical twin cantilevers for single molecule detection

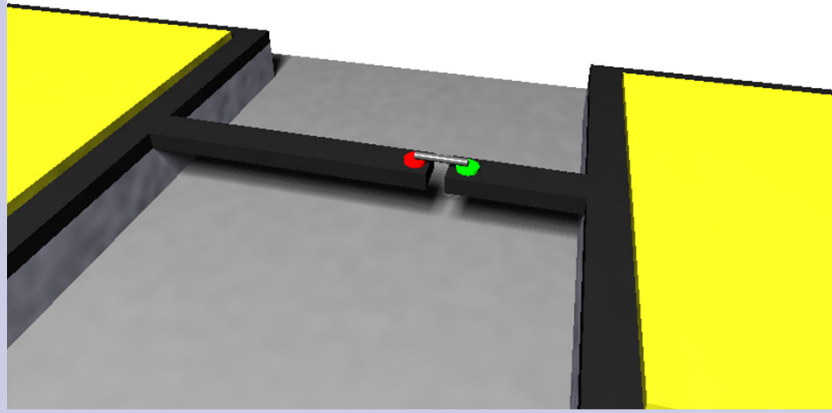
Sergio Carrato

DEEI, University of Trieste, Trieste, Italy

GE 2009
Riunione Annuale

Outline

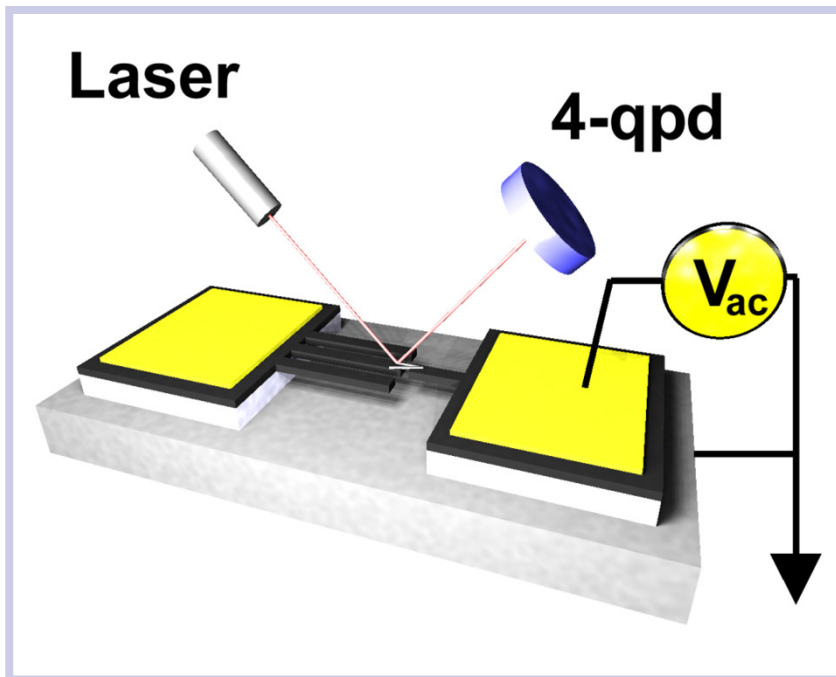
- asymmetrical twin cantilevers
- detection of MW-CNTs
- fabrication of tunable nanometric gap
- selective functionalization of the gap



Asymmetrical twin cantilevers approach

We detect the mechanical cross-talk induced by the molecular link between a short *driver* cantilever and a longer *follower* one.

- The driver is actuated at the eigenfrequency of the follower
- the follower is excited through the molecular link
- motion is optically detected
- actuating force is as low as 0.5 pN with $Q=10000$
- dsDNA is denaturated with a force of about 60 pN



Slide 27

m1

however a second significant technological problem is present. The two cant should be IDENTICAL. Maybe somebody here is as good to do that, but otherwise there are not two degenerate modes, no phase relationship and bla bla bla.

SO why don't fabricate intentionally asymmetric cant.

IN this case we can move the short one, the driver, at the eigenfrequency of the long one and check the motion of the long one. If there is a mechanical link we can see it.

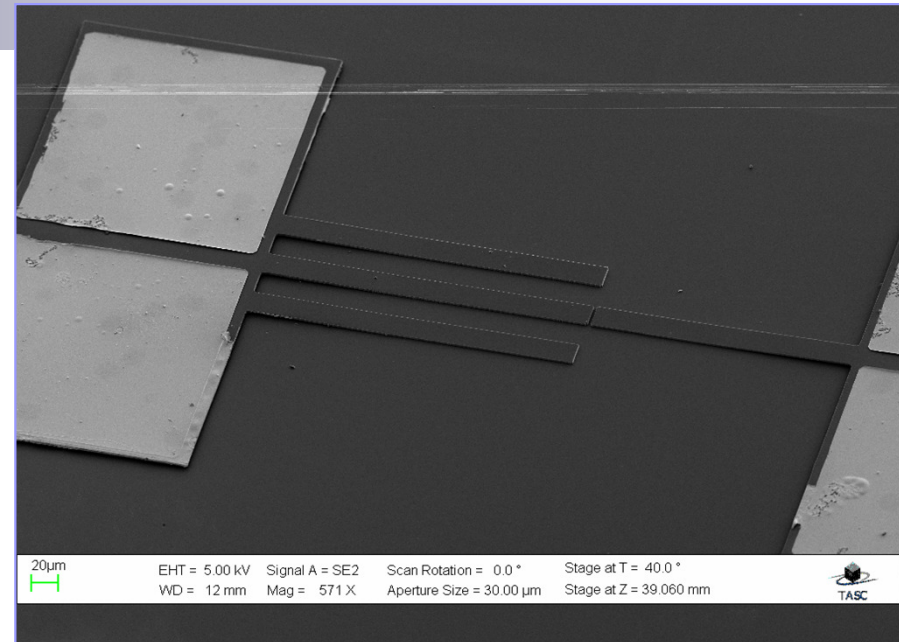
Indeed in spite of the huge mass of the cantilevers with respect to the molecule the force needed to put in resonance a micrometer sized cant can be as low as a fraction of pN - 100 times lower than the force needed to denature a dsDNA molecule.

marco lazzarino; 27/04/2007

Triple *follower* and mode splitting

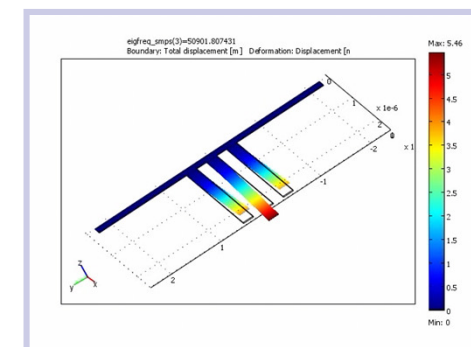
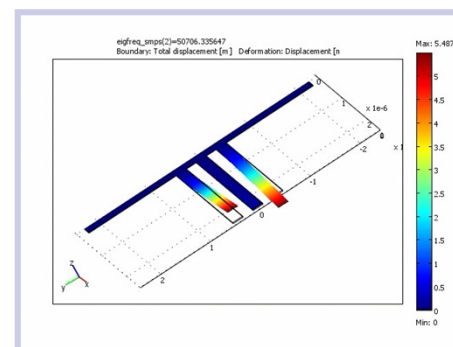
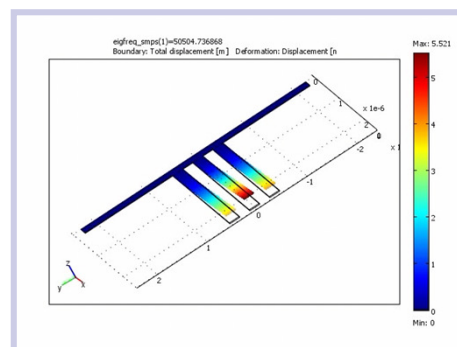
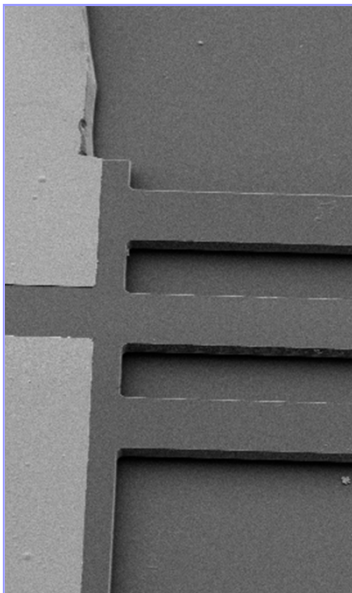
Three nominally identical followers are built

- only the central one faces the driver



The production process causes an undercut that slightly links the three cantilevers

- the three resonators split their eigenfrequency into three modes



Slide 28

m12

we fabricate a device with one driver and three followers.

due to underetch in the suspension process the three are coupled and three modes develop.

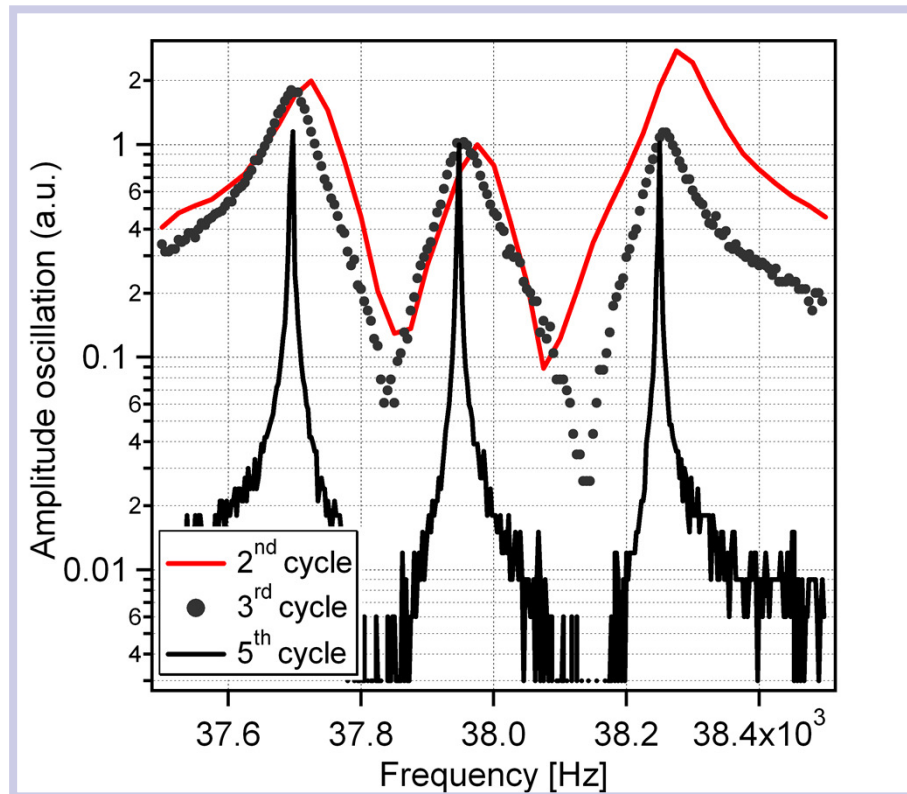
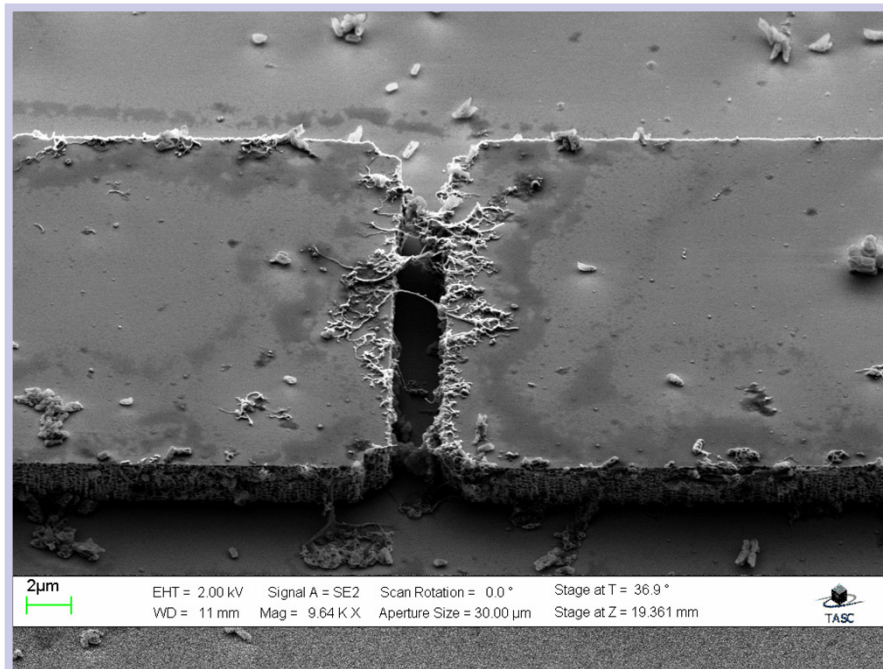
1st, where the three move in phase. 2nd where the central one is at rest and the two lateral move in antiphase and 3rd where the central moves in antiphase with the two external.

we measured optically the motion of the central, self actuated, and as expected the amplitudes are not homogeneous. Indeed the 2nd mode should not be observable but SMALL imperfections, again, break symmetry. However also in this case the third is more than 10 times more intense

marco lazzarino; 27/04/2007

Preliminary tests with MW-CNTs

We placed MW-CNTs as test molecules across the gap by dielectrophoresis



Slide 29

m13

to test our scheme we used MWCNTs molecules, that were deposited only in the gap by dielectrophoresis.
we then actuated electrostatically the driver and detected optically the motion of the follower

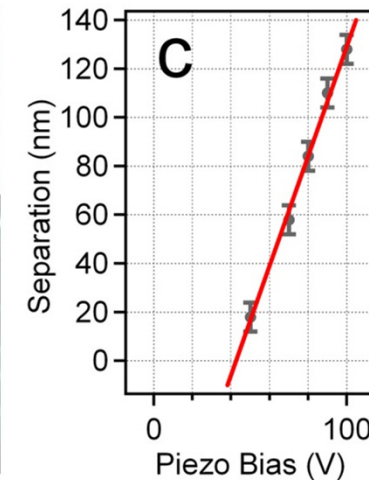
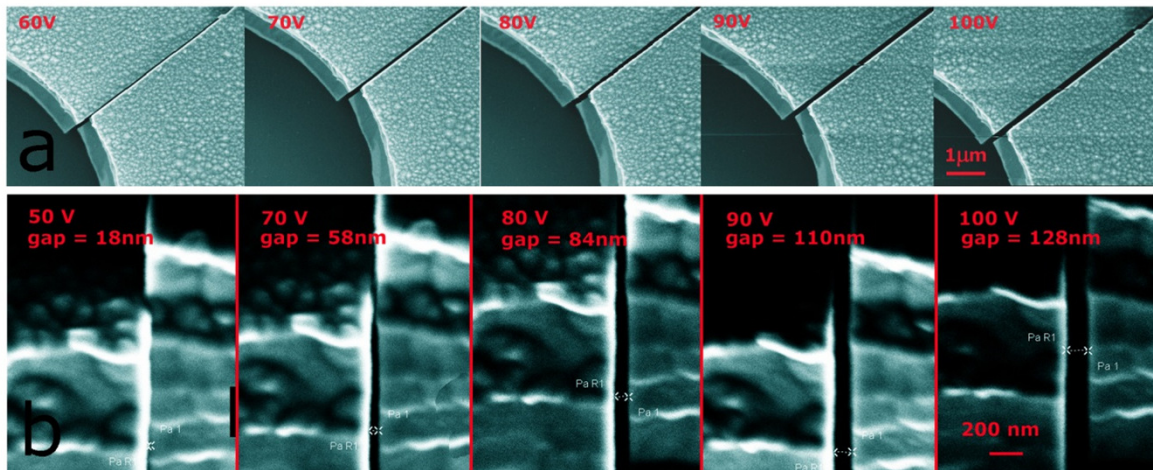
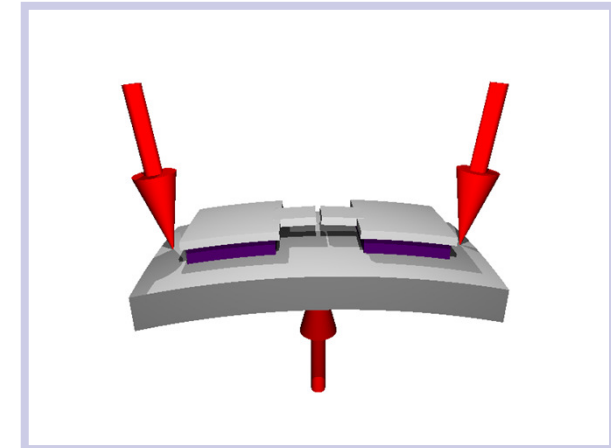
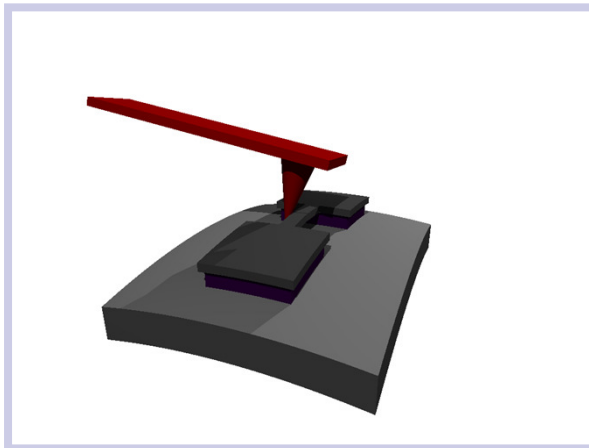
marco lazzarino; 27/04/2007

Gap formation and tuning

For molecular detection we need very flat edges

- the twin cantilevers are cleaved along the $\langle 111 \rangle$ plane by an AFM tip

The nanometric gap is tuned by mechanically bending the whole device



Resolution is 2.2 nm/V

Slide 30

m14

a technological problem for the fabrication of such a device is the creation of a gap of the size of the biological molecule of interest, that should be flat on micrometer scale and, possibly tunable.

We create the gap from a continuous beam, by cleaving along the 111 crystallographic plane of the silicon. To do that we used SOI wafers that offer a single crystalline top silicon layer.

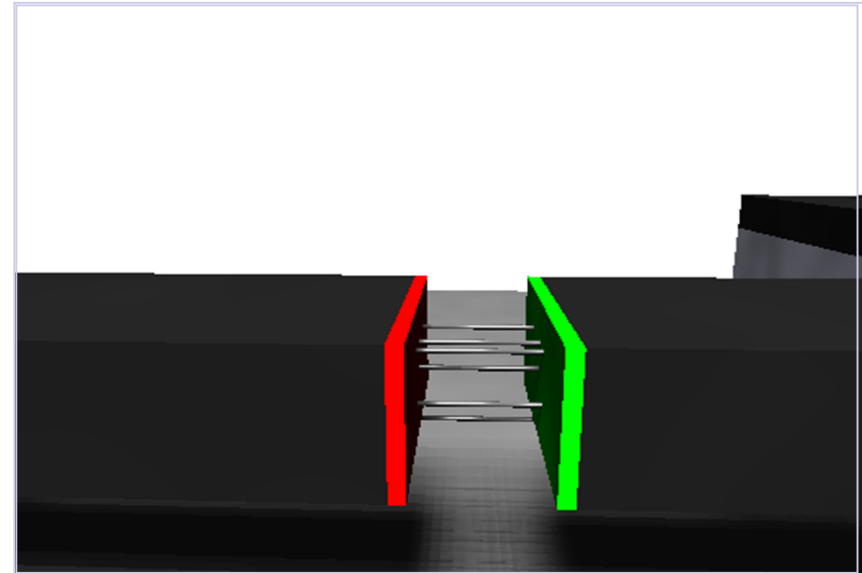
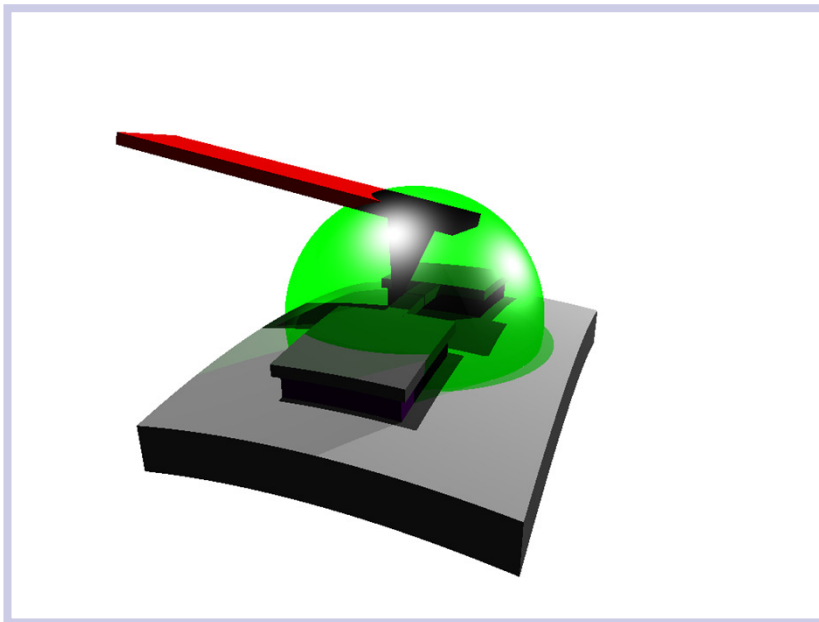
We then tune the gap bending mechanically the wafer in the same way used to generate break junctions.

Our gap is therefore tunable with subnanometric precision

marco lazzarino; 27/04/2007

Spatially defined functionalization

We need to selectively bind the molecules only at the twin cantilever terminations (better if on the facing surfaces)



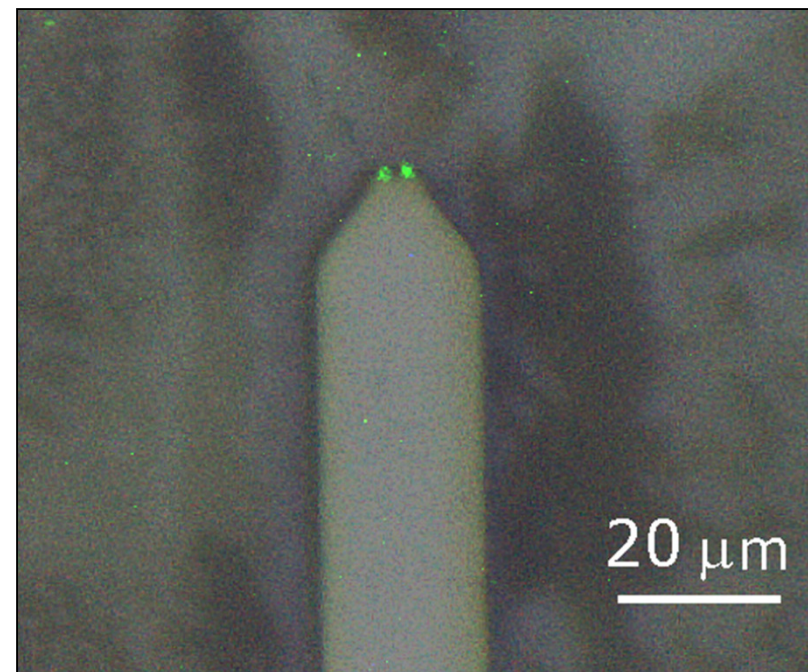
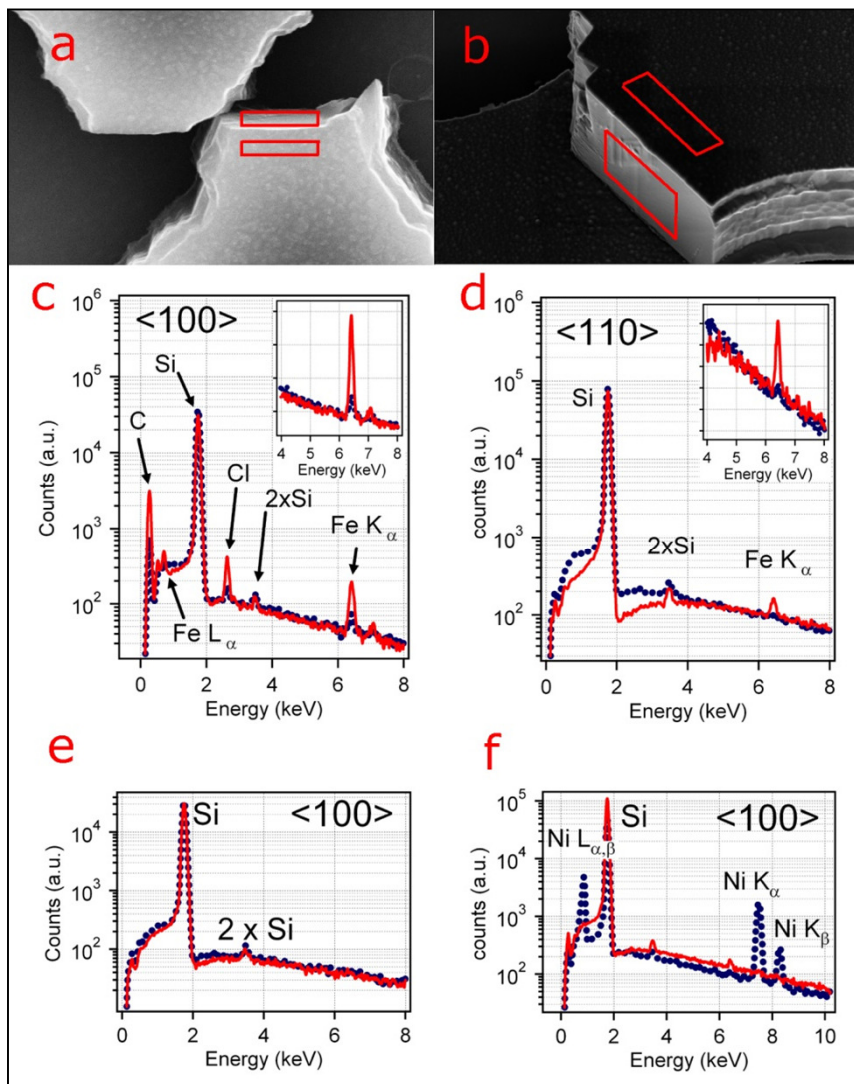
Proposed solution

- cleaving in reactive environment, with no oxidation
- two molecules
 - vinylferrocene
 - fluorescein isothiocyanate (FITC)

Functionalization of the gap

Vinylferrocene solution and SEM-EDX analysis

FITC and fluorescence-optical microscopy analysis



They both reacts only with the freshly exposed Si <111> surfaces



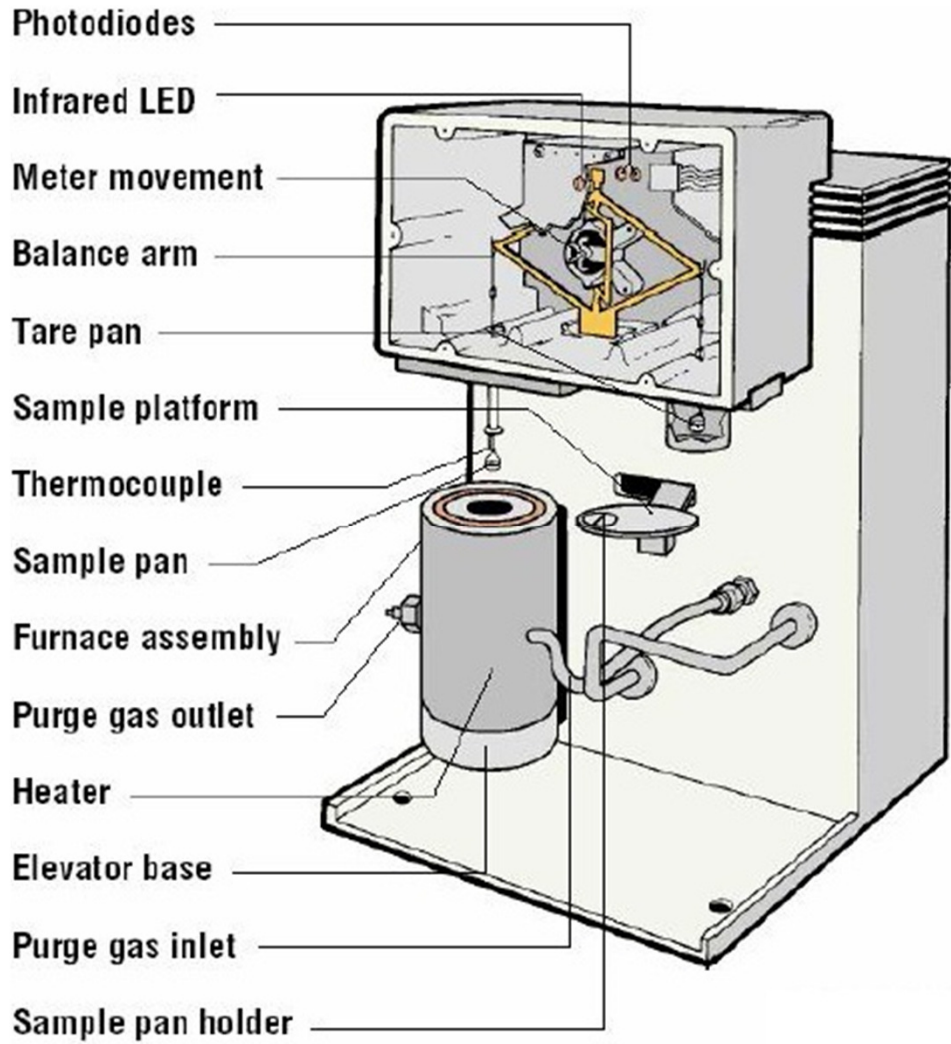
deei



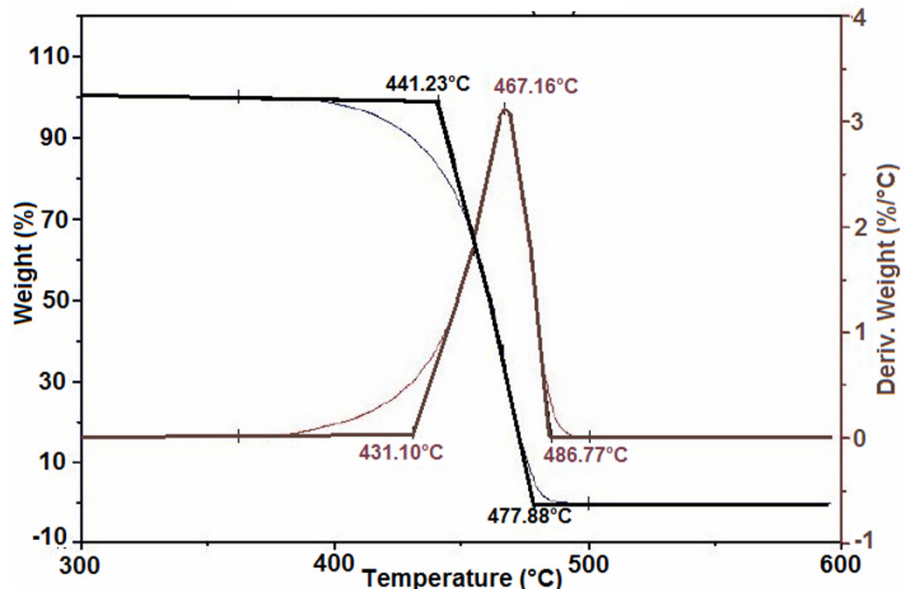
A MEMS based TGA

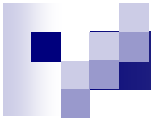
Sergio Carrato
DEEI, University of Trieste, Trieste, Italy

A commercial TGA

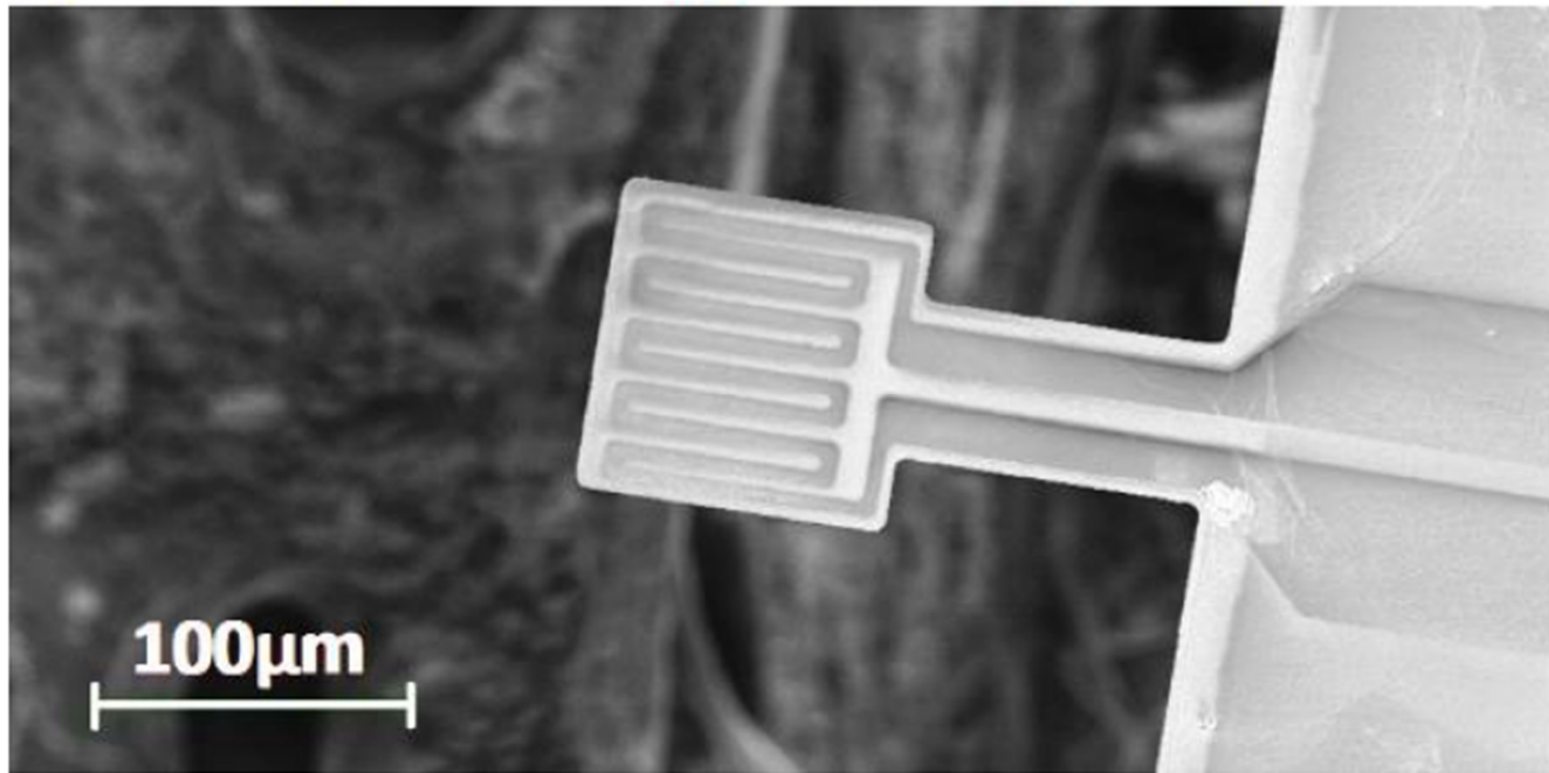


polyethylene

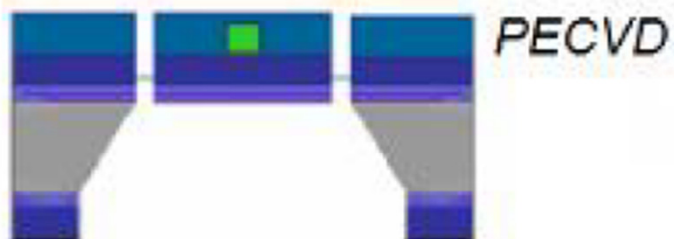
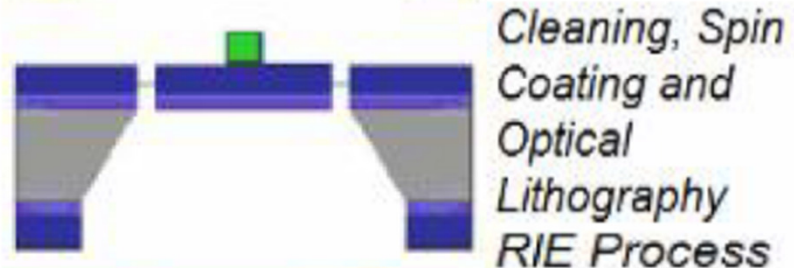
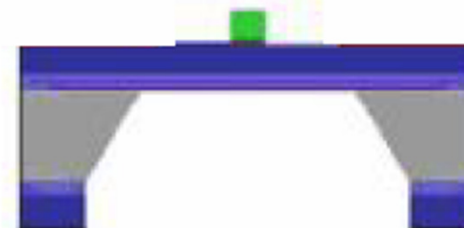
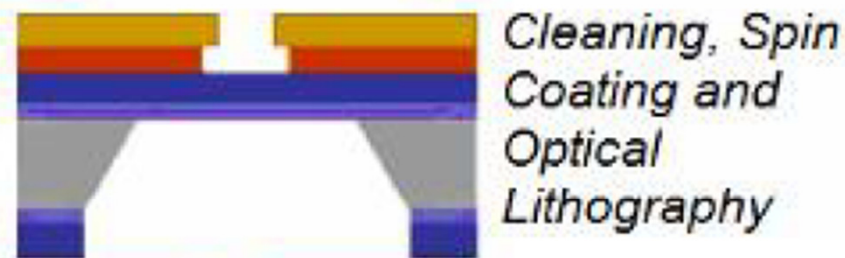
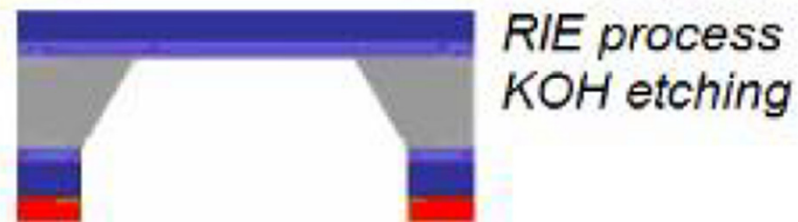
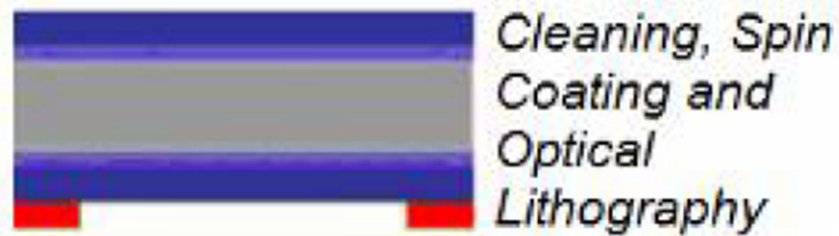




Our TGA

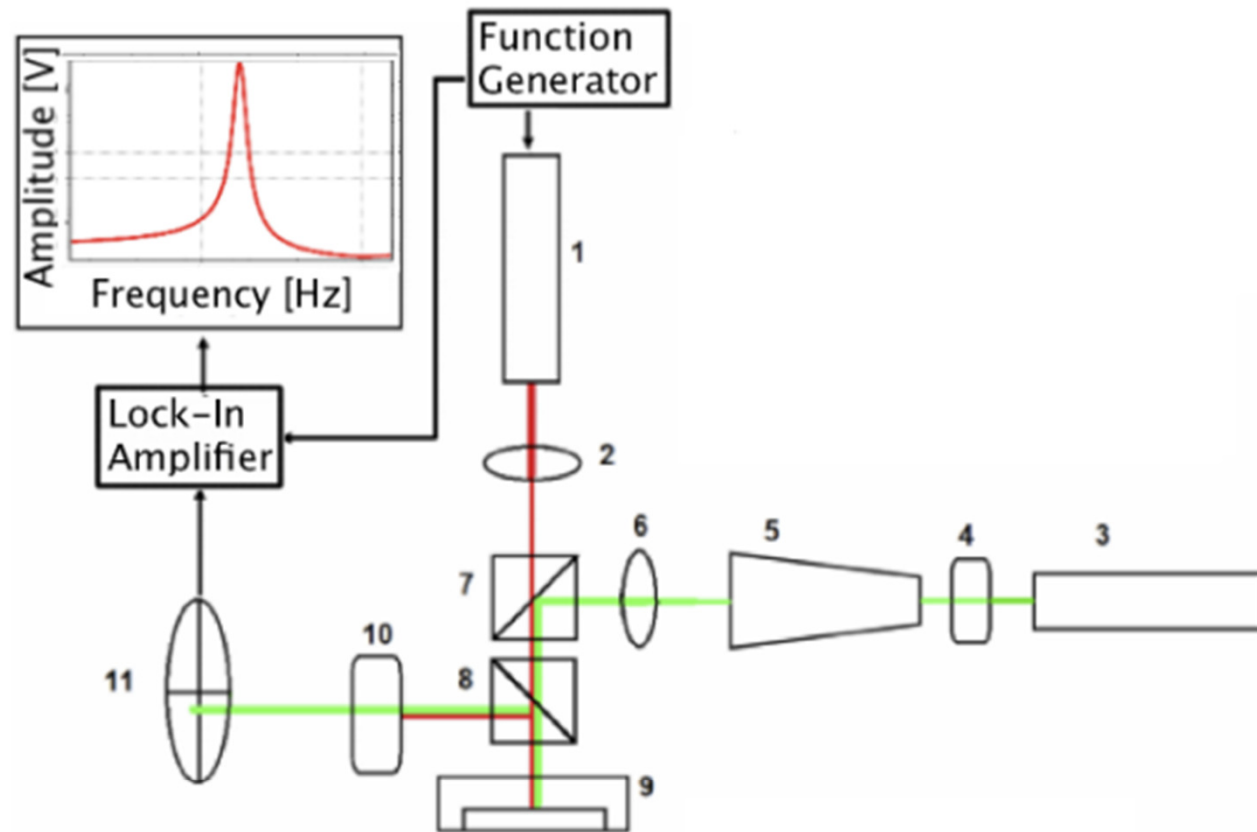


Processing steps



- | | |
|---|---|
|  Silicon |  S1818 |
|  Silicon Oxide |  LOR 3B |
|  Silicon Nitrate |  Nickel |
|  S1828 |  PECVD nitrate |

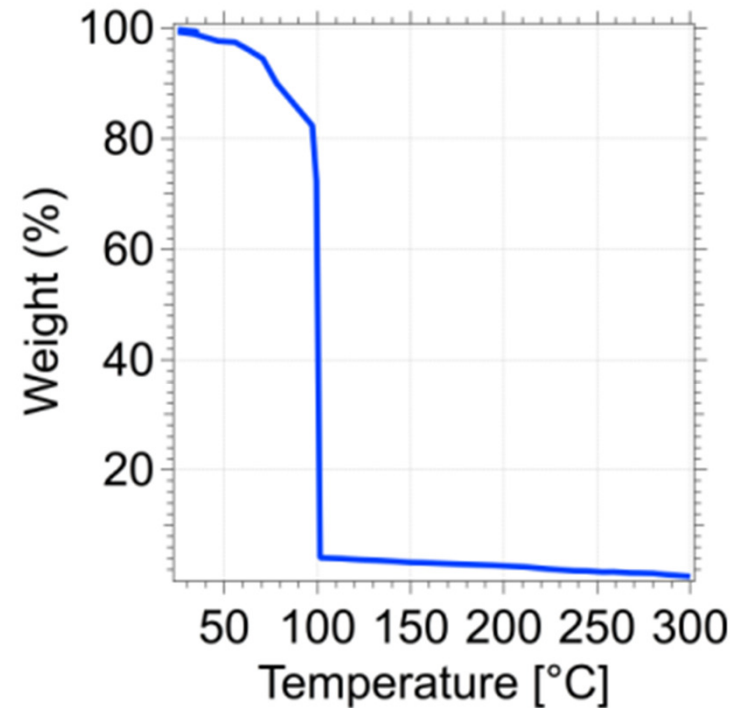
Electronics



- | | |
|------------------------|--------------------|
| 1) Red Pulsed Laser | 7) Beam Splitter |
| 2) Lens | 8) Beam Splitter |
| 3) Green Pulsed Laser | 9) Vacuum Chamber |
| 4) Intensity Modulator | 10) optical Filter |
| 5) Beam Expander | 11) Photodetector |
| 6) Lens | |

Advantages

- Faster heating
- Reduced contaminations
- High sensitivity
- Local heating
- Disposable devices



Test with water

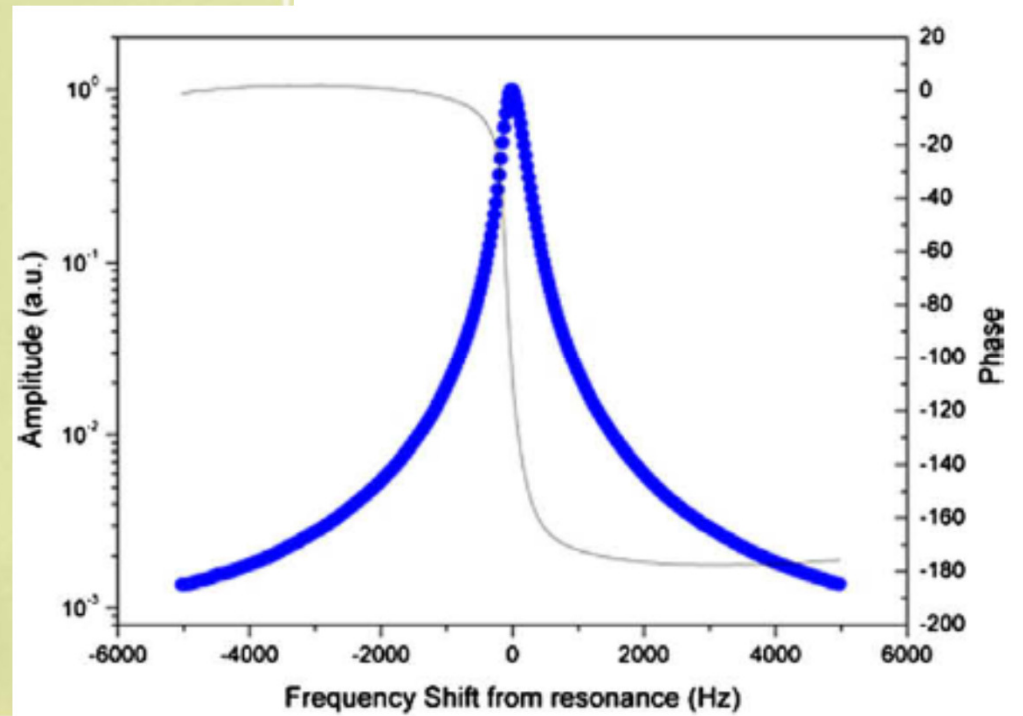
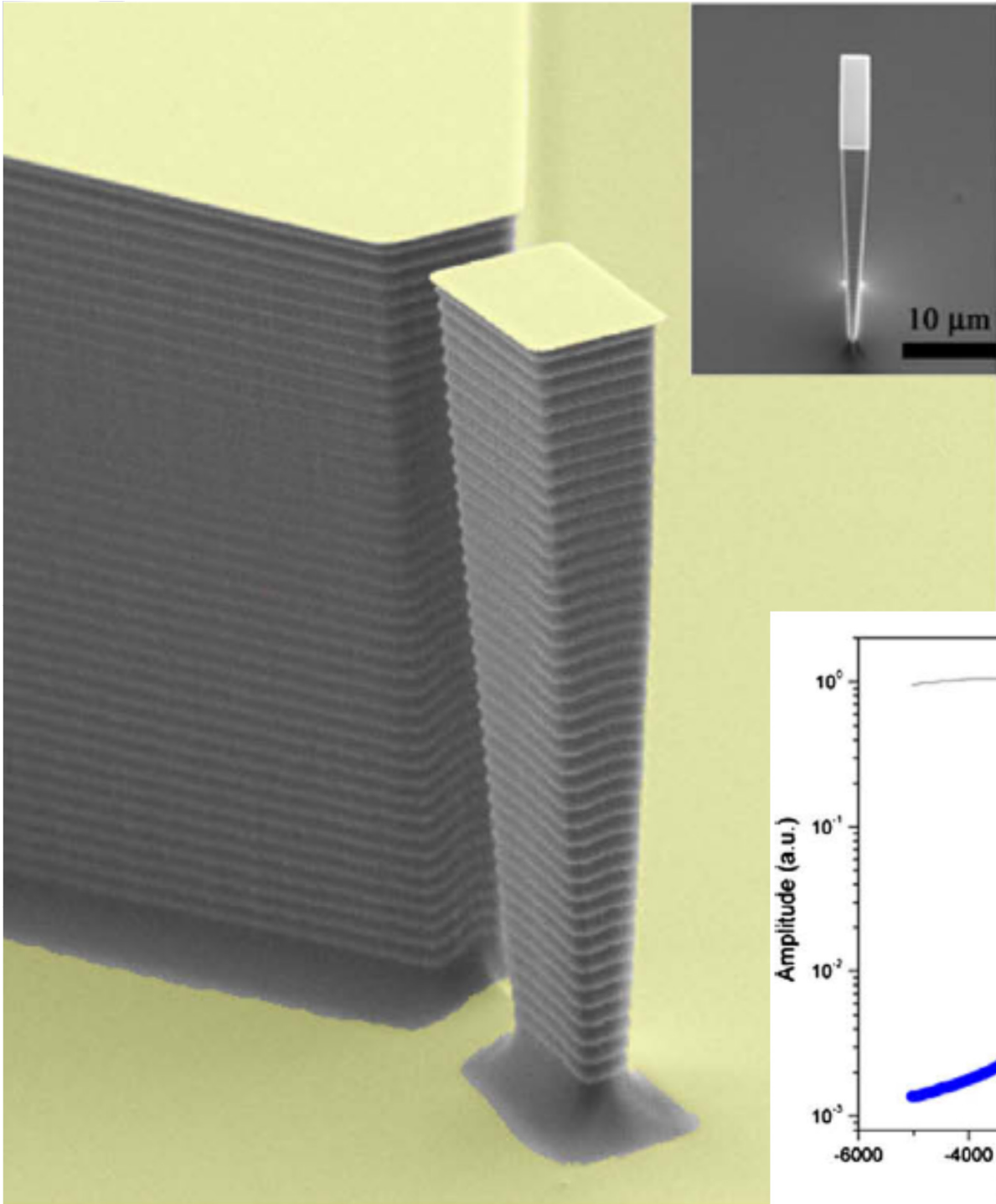


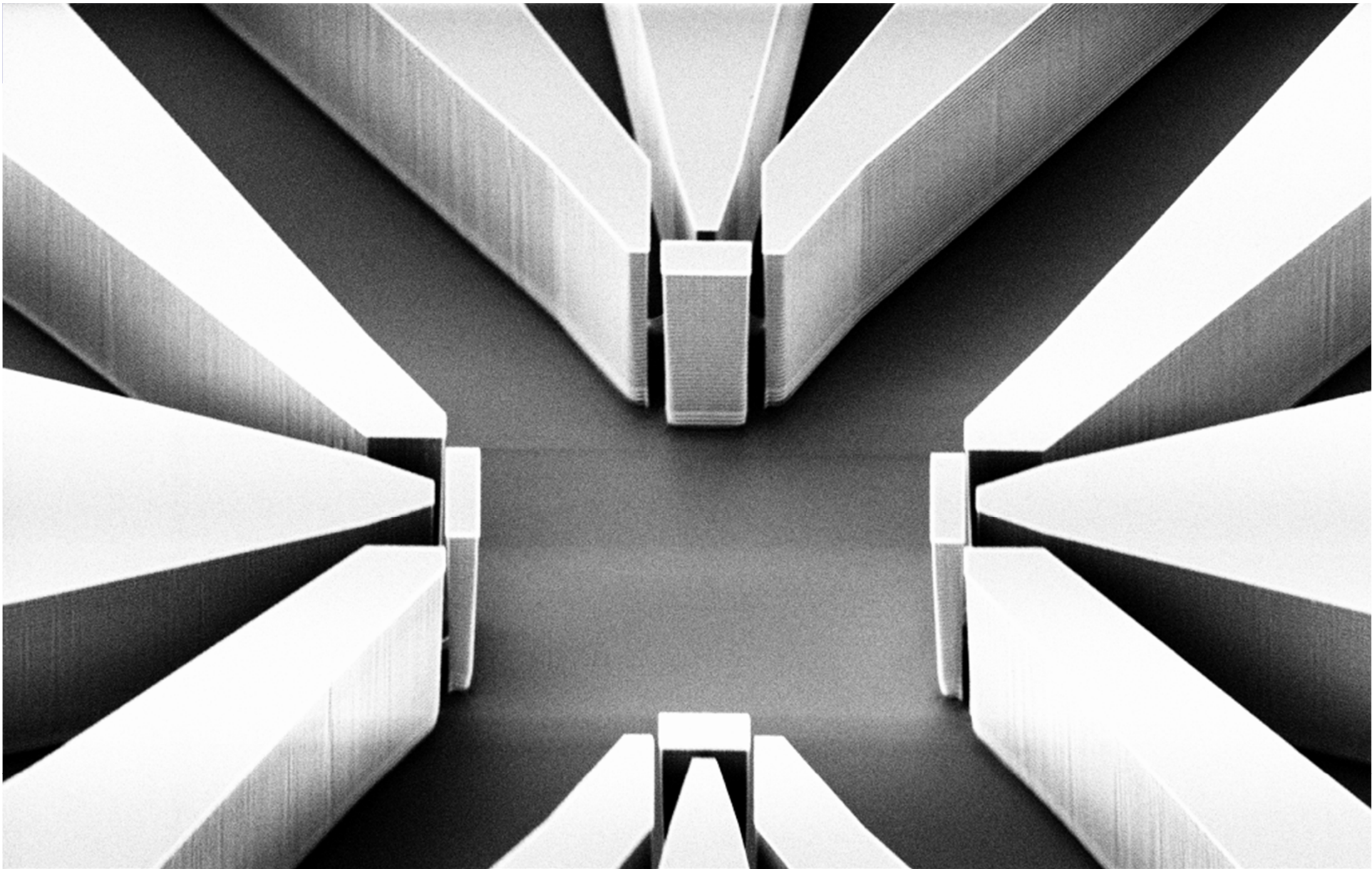
deei



Actuation of silicon pillar micro-
mechanical resonators by Kelvin
polarization force Carrato
DEEI, University of Trieste, Trieste, Italy

Our pillar





LILIT
CNR - IOM

2 μ m



EHT = 4.00 kV

Mag = 947 X

FIB Lock Mags = No

FIB Imaging = SEM

Signal A = SE2

Date :10 Dec 2010

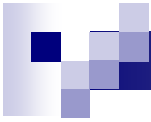
WD = 14 mm

FIB Mag = 246 X

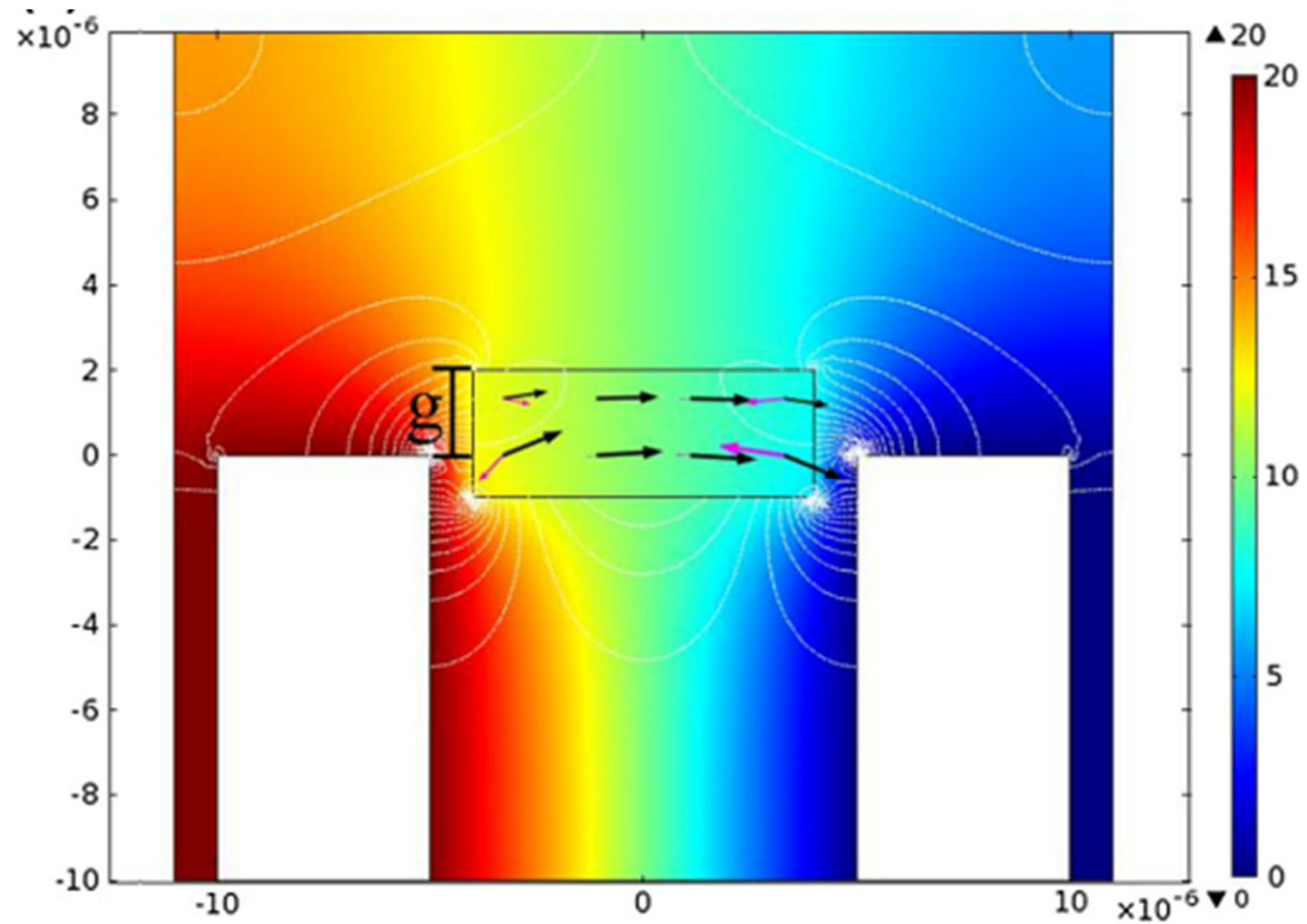
FIB Probe = 500 pA

Signal B = SE2

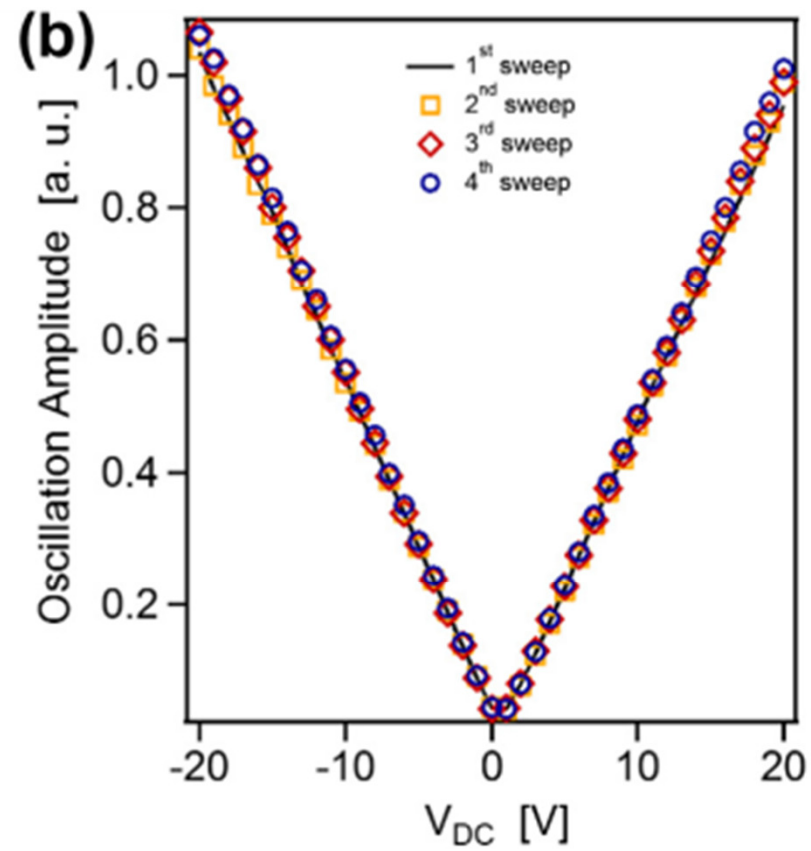
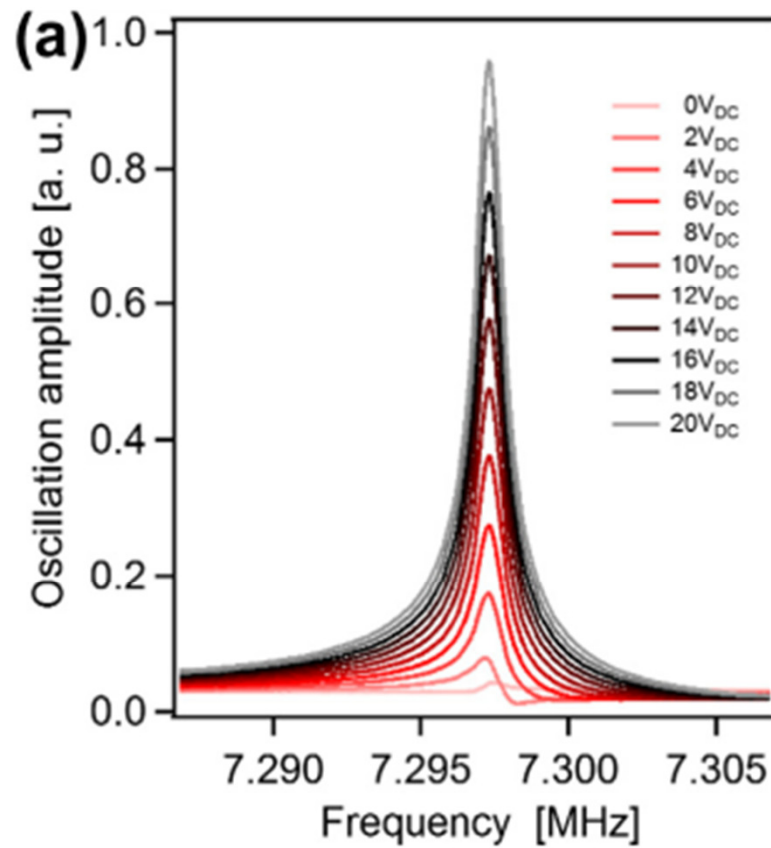
System Vacuum = 1.09e-005 mBar



Electric potential



Resonance amplitude, and dependence on V_{DC}





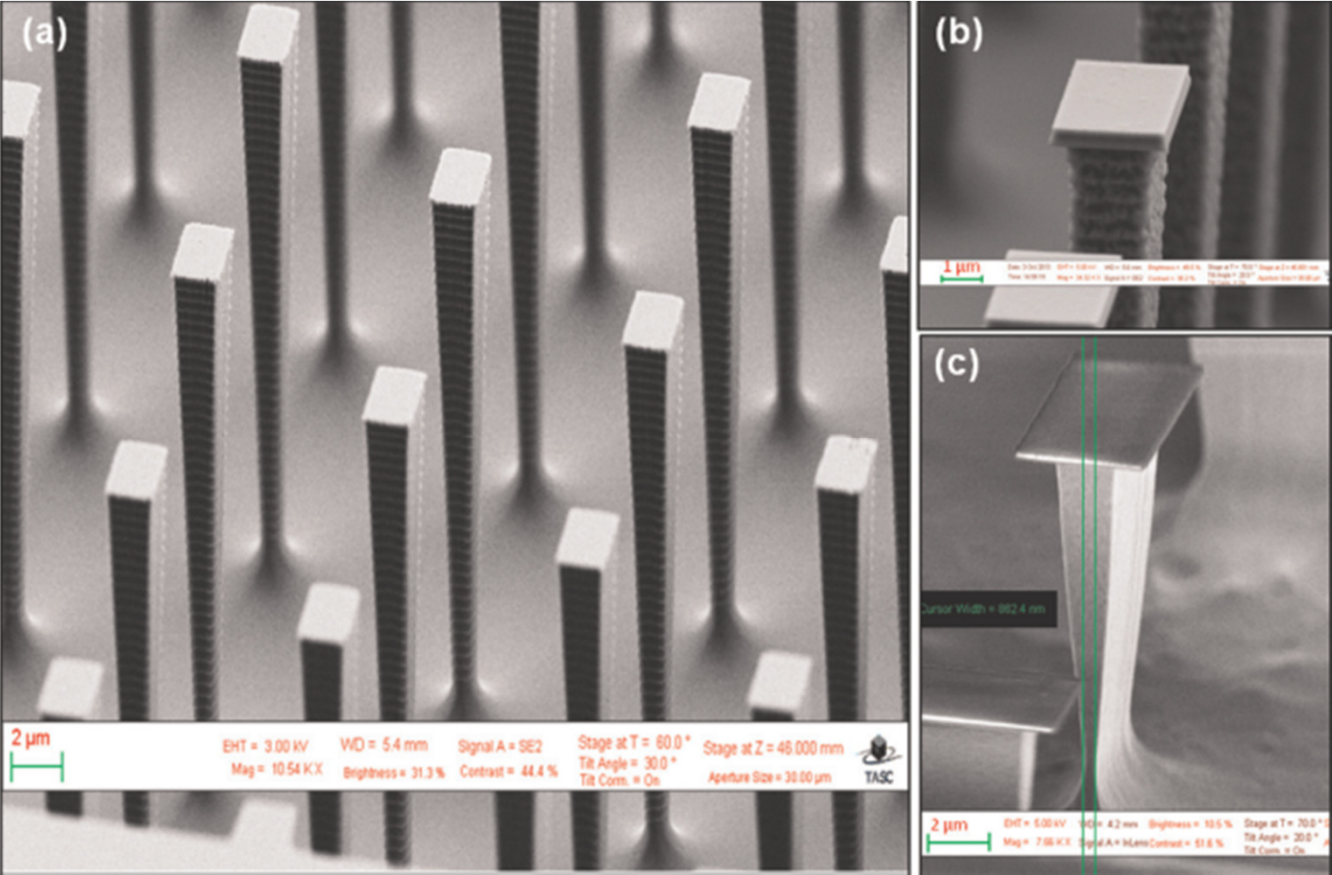
deei



Parallel optical read-out of micromechanical pillars applied to prostate specific membrane antigen detection

DEEI, University of Trieste, Trieste, Italy

SEM image of a micropillars array obtained from deep plasma etching of a patterned silicon wafer



Optical detection of pillar resonance

